tribology in industry
tribologija u industriji

YUISSN 0351-1642
VOLUME 18
MARCH 1996.
1

YU ISSN 0351 - 1642

VOLUME 18
No. 1
MART 1996.

tribologija u industriji

tribology in industry ◊ трибология в промышленности

sadržaj contents содержание

UVODNIK
INTRODUCTION
ВВЕДЕНИЕ

B. IVKOVIĆ: Tribologija - rešenje problema trenja i habanja ◊ Tribology - Solving Friction and Wear Problems ◊ Трибология - решение вопросов трения и изнашивания 3

ISTRAŽIVANJA
RESEARCH
ИССЛЕДОВАНИЯ

A. I. SVIRIDENOK, A. F. KLIMOVICH, V. I. KESTELMAN: Application of Triboelectric Phenomena in Industry ◊ Primena triboelektričnih pojava u industriji ◊ Использование трибоэлектрических явлений в промышленности 5

V. G. BARSUKOV, V. YA. PRUSHAK, V. YA. SHCHERBA, A. I. SVIRIDENOK: The Effect of Friction on The Extrusion of High-filled Composites ◊ Uticaj trenja na istiskivanje visokopunjenih kompozita ◊ Влияние процесса трения на выдавливание высокозаполненных композитов 11

N. N. ANTONESCU, A. C. DRUMEANU, I. NAE: Wear by Thermal Fatigue and Steels Durability from Mechanical Brakes Dry Friction Couplers ◊ Habanje termičkim zamorom i izdržljivost čelika za spregnute delove mehaničkih kočnica izloženih suvom trenju ◊ Изнашивание вследствие термической усталости и стойкости стали для сопряжённых деталей механических тормозов работающих в условиях сухого трения 14

I. BERCEA, N. MITU, I. DAMIAN, M. BERCEA, S. CRETU: A Theoretical and Experimental Study on Friction Losses in a Tapered Roller Bearing ◊ Teorijska i eksperimentalna studija gukitaka usled trenja u kotrljajnim ležajevima sa koničnim valjcima ◊ Теоретический и експериментальный анализы потерь в результате трения в коническо-роликовых подшипниках качения . . . 20

B. ROSIĆ, V. LAĆARAC, M. RISTIVOJEVIĆ: Uticaj raspodele opterećenja na stepen iskorišćenja cilindričnih zupčastih parova ◊ Influence of The Loading Distribution on The Efficiency Ratio of The Cylindrical Tooth Couples ◊ Влияние распределения нагрузки на степень использования цилиндрических зубчатых пар 25

M. ZLATANOVIĆ, A. RAC, D. GERZIĆ, A. KUNOSIĆ: Ispitivanje tribosistema za pumpe visokog pritiska ◊ Testing of The Tribo-systems for High Pressure Pumps ◊ Исследование трибосистем для насосов высокого давления 30

S. PYTKO, S. MARZEC: Quality Estimation of Layers Obtained From A Fluid in The Process of Fine Machining ◊ Procena kvaliteta slojeva dobijenih iz fluida u procesu fine obrade ◊ Оценка качества охладительной жидкости в процессе тонкой обработки

NOVOSTI
NEWS
НОВОСТИ 35

KNJIGE I ČASOPISI
BOOKS AND JOURNALS
КНИГИ И ЖУРНАЛЫ 36

NAUČNI SKUPOVI
SCIENTIFIC MEETINGS
НАУЧНЫЕ СОБРАНИЯ 38

B. IVKOVIĆ

Tribologija - rešenje problema trenja i habanja

10-ti internacionalni kolokvijum o tribologiji

10-ti Internacionalni kolokvijum o tribologiji pod naslovom "***Tribologija - rešenje problema trenja i habanja***" održan je u Esslingen-u, Nemačka od 9 - 11 januara 1996.godine na Tehničkoj akademiji u organizaciji Prof. dr. ing. W. J. Bartz-a.

Na ovoj tradicionalnoj, i u svetu poznatoj naučnoj konferenciji, okupilo se preko 800 naučnih i stručnih radnika iz 40 zemalja. Saopšteno je 225 referata iz svih oblasti tribologije. Uvodne referate na plenarnoj sednici imali su H. P. Jost pod naslovom "***Tribologija - prošlost, sadašnjost i budućnost***", D. Gruden pod naslovom "***Automobilizam izmedju želja i ekoloških zahteva***", C. Kajdaš pod naslovom "***Fizika i hemija tribološkog habanja***" i M. Fuchs pod naslovom "***Svetsko tržište maziva***". Ostali referati bili su rasporedjeni u 28 sekcija koje su se održavale u 6 izvanredno opremljenih sala. Broj referata po sekcijama je bio različit. Najviše referata saopšteno je u sekcijama u kojima su se razmatrali fundamentalni aspekti trenja i habanja (17 referata) i tribološke karakteristike aditiva (22 referata). Tribologiji površinskih slojeva (15 referata) i Tribometriji (16 referata) bila je takođe posvećena velika pažnja.Tribološki aspekt obrade metala rezanjem i sredstva za hlađenje i podmazivanje ramatrani su u dve sekcije u ukupno 26 referata. U posebnim sekcijama razmatrani su Maziva za specijalne namene (9 referata), Bazna ulja (9 referata) i Čvrsta mazaiva sa samopodmazujućim materijalima (12 referata). Sekcije o Kliznim ležajima (8 referata), Podmazivanju kotrljajnih ležajeva (8 referata) i Mazivima za zupčaste prenosnike (11 referata) bile su dobro posećene za sve vreme trajanja konferencije. Veliki broj učesnika bio je zainteresovan za Ekološki aspekt maziva (10 referata), problematiku Mešanog podmazivanja(12 referata), Podmazivanje mastima (7 referata), Motorna ulja (9 referata) i Ispitivanju motornih ulja (6 referata). U sekcijama u kojima su razmatrani Tribološko ponašanje materijala, Tribološko ponašanje plastičnih materijala i Tribološke karakteristike materijala saopšteno je ukupno 19 referata.

Posebnu pažnju privukli su referati saopšteni u sekciji Tribologija veštačkih kukova, koja je praćena i izložbom tribomaterijala koji se u ovoj oblasti koriste, kao i brojnim tipovima konstrukcije veštačkih kukova.

Posebna sekcija bila je organizovana za izlaganje radova proizašlih iz tribioloških istraživanja ostvarenih poslednjih godina u Nižnjem Novgorodu, Rusija. Referati u ovoj sekciji su bili teorijsko-eksperimentalnog karaktera i odnosili su se, uglavnom, na fundamentalni aspekt problema trenja i habanja.

Manji broj referata saopštenih na ovoj konferenciji odnosio se na Tribologiju zaptivki, Hidraulična ulja i Maziva u obradi deformisanjem.

Iz Jugoslavije na konferenciji je saopšteno tri referata. Jedan se odnosio na Tribologiju rezanja (Mašinski fakultet u Kragujevcu), a druga dva na tribološke karakteristike površinskih slojeva formiranih plazmom (Fakultet tehničkih nauka, Novi Sad).

Konferencija je ocenjena kao izuzetno uspešna, kako po broju saopštenih radova i njihovom kvalitetu, tako i po ukupnom broju učesnika. Veoma je malo naučnih konferencija iz oblasti tribologije u svetu koje okupljaju ovako veliki broj učesnika, posebno učesnika bez referata. Kotizacija od 850 DM za učesnike bez referata nije bila prepreka da preko 600 naučnih i stručnih radnika iz, uglavnom, nemačke industrije prisustvuje konferenciji. Zapaženo je da su za sve vreme trajanja konferecije sale u kojima su

izlagani referati bile pune. Ovako veliki broj učesnika iz nemačke industrije ukazuje na njihovo shvatanje o potrebi neprekidnog inoviranja znanja i prikupljanja novih informacija tribološkog karaktera koje mogu da doprinesu smanjenju troškova proizvodnje i povećanju konkurentske sposobnosti na tržištu.

Za vreme trajanja Konferencije bila je organizovana i izložba tribometara više proizvodjača, uredjaja za regeneracuju sredstava za hladjenje i podmazivanje, tribomaterijala i veštačkih kukova različite konstrukcije.

Tribometar firme WAZAU izgrađen na osnovu istraživačkih iskustava u BAM-u i sa njihovom dozvolom, prikazan na izložbi, omogućava ostvarivanje sve tri vrste kontakta (u tački, po liniji i po površini) i predstavlja jedan od članova familije tribometara ove vrste. Posebnu pažnju izazvao je i Tribometar za ispitivanje triboloških procesa u uslovima fretinga.

Pored izložbe tribometara i druge instrumentacije, organizovane u prizemlju zgrade Tehničke akademije, u prostorima ispred sala u kojima su se izlagala saopštenja bio je izložen prospektni materijal brojnih triboloških časopisa koji su štampani, uglavnom, na engleskom jeziku.

Tribology - Solving Friction and Wear Problems

10th International Colloquium on Tribology

The tenth International Colloquium on Tribology entitled Solving Friction and Wear Problems was held at Esslingen , Germany, on 9 - 11 January 1996. at Technical Academy, in organization of Prof. dr. Ing. W. J. Bartz. The Conference was attended by over 800 of participants from 40 countries, and 225 papers were presented from almost all fields of tribology.

Apart from the standard tribological problems, the ecological aspect of lubricants and application of synthetic materials, were considered to much larger extent, than on earlier meetings. The largest number of presentations was from the area of tribology of cutting, additives, tribology of surface layers and tribometry.

During the Conference were organized exhibitions of tribometers, devices for regeneration of coolants and lubricants, tribomaterials, artificial hips, and publishing activities from the area of tribology.

Трибология - решение вопросов трения и изнашивания

10-й международный зачёт по трибологии

Десятый Международный зачёт о трибологии под названием "Трибология - решение вопросов трения и изнашивания", состоялся с 9 по 11 января в городе Эслинген, на Технической академии, в организации др. техн. наук, профессора В. Бартца. На собрании участвовало более 800 специалистов из 40 стран. Участники настоящего триболгического собрания выступили с 225 докладами почти по всем областям трибологии.

Наряду с стандартными вопросами трибологии, рассматривались, в большей мере чем до сих пор, экологические асиекты применения смазок и использования пластмассовых материалов. Большинство работ касалось вопросов трибологии резания, использования присадок, трибологии покрытий и трибометрии.

В течение собрания были организованы выставки трибометров, установок для восстановления СОЖ, трибологических материалов, искуственных суставов и публицистической деятельности в области трибологии

UDK 620.93.003.1:621.891

A. I. SVIRIDENOK, A. F. KLIMOVICH,
V. I. KESTELMAN

Application of Triboelectric Phenomena in Industry

1. INTRODUCTION

At production, processing, and operation, polymers are undergoing intensive mechanical, electromagnetic, and other physical forces, which followed by deformation and destruction of contacting bodies. At the same time a structure and physical features of interacting surfaces are changed essentially. The change of electro-physical features is a striking display of those changes.

In spite of long investigation history of the material electrification an effect of the contact electrification and the electret state on friction and wear of polymers has been scantily studied [1]. As a result, there is a lack of practical knowledge of tribology and its application.

It is known that the electrification takes place at any friction and for any contacting bodies including solid, liquid, and gaseous state, therefore, the contemporary physical model of the condensed media electrification is based on conception of surface states [2]. This conception is very important for studying a mechanism of the frictional electrification of polymers. Electrophysical, physical-and-chemical processes and structure changes in disperse polymers at tribo-mechanical undergoing are the most typical examples. Under those conditions the long-life electret state has been identified. The important role of temperature in determining the interaction between structure changes of polymer particles, their morphology transformation, and an intensity of the contact electrification was shown.

Results of studying of the electrification effect on the friction between sectional polymers taking into account adhesional, kinetic, and electret aspects are of great interest. The generation of the electret state is a result of the electrification at frictional contacts not only between polymers but also between polymer composites.

Natural and particularly artificial electret state effects essentially the friction and wear parameters due to, first of all, the transformation of a super-molecular structure and the electret- and triboelectrification superposition.

The acquired knowledge was used at a development of new form of electrets, polyelectrets. For those polyelectrets the great enough charges, long-lived, were obtained. For example, fillers, entered into the polymer, effect on electrophysical and tribologic features of composites at friction. The electret filler can increase or decrease the electromagnetic field generated at the friction contact, i.e., one can realize the conception of the electret- and triboelectrification composition. The electret phenomena are displayed distinctly at friction in vacuum and liquids for dielectrics, as well as for electrolytes.

A current inversion, registered at friction of polar and nonpolar polymers for disperse and sectional samples, is a general dependence of the electrification at friction of polymers and polymer composites.

A mechanism of the electrification and the generation of the electret state at polymer friction has been proposed. The mechanism was based on general conceptions of the electric theory of disoriented systems and surface states. It allowed to substantiate the conception of the unity and the common character of the electrification and the electretization at friction contact of polymers and polymer-based composites, to summarize contemporary knowledge in the field of electrophysics of the polymer friction [1].

Anatoly I. Sviridenok, Albina F. Klimovich,
Academy of Sciences, Belarus
Vladimir I. Kestelman,
ITP, USA

Two directions should be considered that are application of positive effects of those phenomena and prevention of negative effects. Historically directions connected with electrification were developed firstly, then in '80s those were connected with the electret phenomenon.

2. METAL-AND-POLYMER FRICTION UNITS

The most widely, electric phenomena are used to control friction parameters of polymer-metal contacts. It is carried out with aim to suppress triboelectricity in different ways: combining plastics of different polarity, passing a current, encasing the plastic electro-conductance or by previous electrification. Triboelectric phenomena play an important role in charge-alternating and choosing transfer, friction saturation by hydrogen.

The method of suppressing static electricity by passing a current to decrease a triboelectrical component is the oldest one [3]. For example, a friction moment for a pair steel - fabric-based-laminate is decreased at every switching of a discharger by 40% (a temperature of units being under friction is decreased too).

One of the methods for suppressing the static electricity is a combination of electropositive E^+ and electronegative E^- plastics at units production. The total electric charge is decreased in this case. The minimum electrification was obtained for a shaft made from 60 - 70% of polymethyl-methyl-metacrylate (electronegative plastic) and 40 - 30% of fluoroplastic (electropositive plastic).

The friction moment is decreased, reaching the optimal values when the content of electronegative and electropositive plastic are approximately the same. To suppress momentary discharge pulses, the composites made from plastics with addition of electro-conducting fillers, i.e., graphite, carbon-black, metal powders, are applied and then a current is passed through the contact. On suppressing the triboelectricity, the decreasing of friction moments of pairs by 9 - 10 times, as well as improving of antifriction features of conjugates, were marked out. There is "a spreading" metal with antifrictional plastics at their positive charging (electropositive plastics) and metalizing plastics at their negative charging (electronegative those). An abatement of electrification, as well as decreasing of the friction moment and the temperature of units, conjugated associate the combination of electropositive and electronegative plastics. On increasing the electric conductance of polymers, e.g., at making graphite, carbon-black, disperse metals, etc. a part of polymer, the total potential is decreased too. For example, on adding 50 weight units of graphite to epoxy resin the potential falls from 2000 V to 400-500 V, and on adding 100 weight units of graphite it goes to 50-100 V.

In the work, the connection of surface conductance changes with a wear of polymers was marked too. The author of the work [3] associates the decreasing of a polymer ability to generate and to accumulate the static electricity at increasing their conductance with the decreasing of number and the surfaces of contact spots between polymer and metal (due to creation, inside polymer, of space structures in the form of chains made from the electric conducting filler). The three-component system metal-filler-polymer is formed that is notable for increasing discreteness of polymer-metal contact. The total potential decreases also as a result of leakage due to the high conductance. On increasing conductance, the potential decreases, but the current, drawn from one body being under friction to another, increases. A lubricant decreases abruptly the electrification of bodies rubbed, too, and the higher electric conductance the sooner is the effect.

In that way, the friction of metal-polymer pairs is accompanied by the essential electrification, an intensity of which is determined by the chemical and physical nature of bodies. The suppressing of charges generated is accompanied by decreasing the friction moment by 80-90%, as well as by decreasing the temperature of units rubbed. The wear of those units depends on a direction of the electron movement in the contact zone. In this case, the unit losing electrons is worn out firstly.

A negative display of the static electrification at function of the metal-polymer friction unit is connected, by authors of the work [4], with the hydrogen wear. It is known that hydrogen releasing at the plastic friction leads to the hydrogen saturation and to an embrittlement of the steel surface [5]. At the same time, just the triboelectrification promotes the penetration of proton, which has a small dimension of about $1 \cdot 10^{-13}$ cm, into metal lattice, which has an opposite charge. In this case there is an interconnection between the charge sign of the polymer friction surface and the saturation by hydrogen. The polar charging corresponds to increasing by 2-3 times of the percentage of hydrogen.

In addition to the list of the negative displays of the accumulation of the static electricity in tribo-conjugates, one can note that electrically charged plastic surfaces can attract from the environment dust, moisture, wear particles of the counterbody; at drawing together with metal bodies grounded there could be discharges, electric ageing of plastics and the metal electric erosion. To prevent the accumulation of electric charges, it is necessary to decrease the plastic resistivity to 10^6 Ωcm and less. It is achieved by application of electric conducting polymer composites and lubrications.

The application of electret phenomena for the control of friction features of polymer in units of sliding friction with negligible heat emission was started. The control is carried out as a result of the electrostatic interaction

between the space charge, generated at the polymer electrification, and the space tribo-charge friction generated. In this case, depending on the sign of the electret charge and the tribo-charge, there is possible increasing as well as decreasing of the coefficient of friction and of the wear intensity of polymer comparing with the initial state.

In Table 1 the dependence of the friction force F and the mass wear intensity J_g on the magnitude and the sign of the effective surface charge density of covers thermo-electrified (ESCD) are shown.

Depending on the magnitude and the sign of the charge previously formed, the electrification of covers leads to decreasing the friction force by 10-30% and the wear intensity by 1.5-3 times. This feature is important at starting and run-in.

Table 1. Changes of the friction force F and the wear intensity J_g of thermo-electrified covers

Covers					
Polyethylene			Polycaproamide		
ESCD mkC/m²	F,N	J_g mg/M²m	ESCD mkC/m2	F,N	J_g mg/M²m
0	3.5	1.35	0	2.9	3.87
+10	3.3	0.78	+1.6	2.7	2.32
+20	3.0	0.68	+6.0	2.1	2.70
+40	3.1	0.55	+13	2.1	3.47
+60	3.3	1.08	+20	3.0	-
-10	3.6	1.01	-1	2.9	1.88
-20	3.5	0.87	-3	2.8	1.86
-40	3.6	0.49	-8	2.2	-
-60	3.8	1.01	-20	2.8	-

In this way, the initial electrification could be an effective method to control friction features of polymers.

3. DIAMONDS PROCESSING

The new field of the electret application is a use of polymer electrets in processing of diamonds [6]. It is known that diamond is a dielectric with an electric resistivity of 10^{12}-10^{14} Ωm and a dielectric constant $\varepsilon = 5.7$. As a result, diamonds accumulate great electric charges during friction. Having unique features, diamond is one of the most difficult materials to process.

Diamond crystals are sawed by the special machine-tool with thin disks made from tin-phosphorus bronze and charged by the diamond powder. A destruction of diamonds at sawing is a result of the dynamic contact between the diamond crystal and the edge of the sawing disk. At the angular velocity of the spindle about 10 000-14 000 rpm and the disk diameter of 65-76 mm the linear velocity on the disk edge is 35-55 m/s. The dynamic contacting of metal-dielectric systems is accompanied by the intensive electrification that is proved at diamond sawing (Table 2).

Table 2. Electrification current at diamond sawing by disks with different covers

Bind of the disk's diamond layer	Electrification current nA	
	Polarity	Abs. value
Disk charged	+	10-30
Petroleum oil	+	10-20
Copper-zinc alloy electroplating	+	40-60
Nickel electroplating	+	100-120
Polytetrafluorethylene	-	30-40
Polycrylonitrile	+	100-130
Polystyrene	+	200-300
Polyamide resin	+	200-300
Phenolformaldehyde resin	+	300-500
Polyamide resin modified by graphite and molybdenum disulphide	+	200-350

At sawing by disks uncharged and disks with a bind made from the castor oil the electrification current is 10-30 nA. The current increases at sawing by disks with electroplating: by 2-3 times in the case of nickel electroplating, and by 5-6 times in the case of copper-zinc one. Using polymers as a binder leads to abrupt increasing of the current of electrification and the polytetrafluorethylene-binder changes the polarity from positive to negative. As it could be seen from data presented, the value of the current of electrification at application of polyamide resin, polystyrene, and phenolformaldehyde resin is about 200-500 nA and more. The potential of arbour in this case mounts to 200 V.

In Fig. 1 are shown kinetic curves of the current of electrifcation at sawing diamond crystals by uncharged

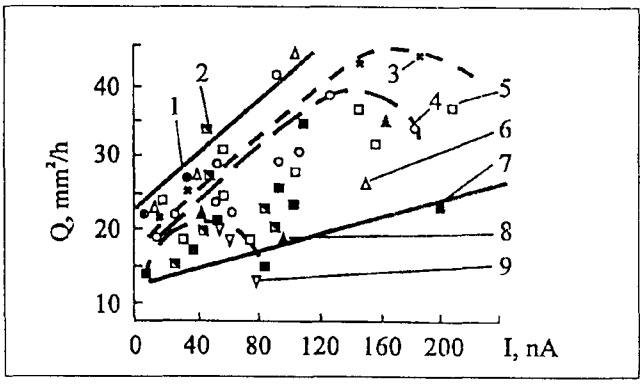

Fig.1. Dependence of saw productivity versus the average current of electrification in the case of the sawing disks charged by different diamond content compositions: I, castor oil; 2, polytetrafluorethylene; 3, polyamide resin modified by graphite and MoS_2; 4, polyamide resin; 5, phenolformaldehyde resin; 6, polyamide- and phenolformaldehyde resin; 7, polystyrene; 8, polyamide-and polystyrene resin; 9, polycrylonitrile.

disks, serial disks with binder from the castor oil, and disks with the polyamide resin binder. For all binders the kinetic curves of the current of electrification have extremum due to specific character of diamond sawing that is gradual cutting-in crystal, the contact surface increasing and following decreasing of it.

With aim to elucidate an interconnection between the current of electrification generated, the speed of saw and the disk firmness comparing tests were carried out on serial disks at connection and disconnection of disk and crystal to ground. The tests displayed that the complete insulation leads to abrupt fall down of the current of electrification and decreasing the speed of saw by 18-20%. The firmness of disks increases in this case by 2 times. On analyzing the test results one can summarize that the high productivity tool should have the wear-steady high-electrifying binder and the attachment of crystal and tools should be grounded.

In Table 3 data, showing an effect of polymer binder in diamond-content layer on the main parameters of the saw of diamonds, are presented.

Table 3. Sawing of diamond crystals

Binder of diamond-content layer	Current of electrification I [nA]	Saw intensity Q [mm²/h]	Losses [%]	Processing quality
Castor oil	+30	18.14	9	Good
Polyamide resin	+280	20.18	7	High
Polyamide resin modified by graphite and molybdenum disulphide	+320	21.05	6	Very high

Investigation data show that the electrification intensity, which is determined by the current of electrification, is connected with the speed of saw, the disk firmness, and the quality of semifinished items [7].

There is a negative aspect of the effect of the electric current on the saw of diamonds besides positive one. That is the decreasing of the tool firmness. For example, at the current of electrification of 0.5 (for tools electrically insulated), 25 and 80 nA the average firmness of disks charged by the castor oil is 305, 190 and 153 mm^2 correspondingly. As a result, at high magnitudes of the current there could be seen the productivity decreasing due to worsening of saw-features of the disk.

A dependence of the saw productivity on the current of electrification for the tool charged by serial (castor oil) and by composition way (polyamide resin with addition of phenolformaldehyde, graphite and MoS_2) is presented in Fig. 2. The dependencies were registered at processing of identical crystals of diamond at the same conditions: the working load of 1.2 N and the rotation speed of the disk of 13 000 rpm. The duration of saw t [min], the surface of sawing S [mm^2] and the saw quality judged by eye were registered in those experiments.

Table 4. Dependence of saw intensity on method with and without electret washers

Disks	Saw method	Crystal mass, [carats]	Saw intensity Q [m²/h]	Processing quality
With Castor oil	With electret washers	0.46-0.53	19.646	High
		0.25-0.30	19.068	
	Without	0.46-0.53	18.191	Good
		0.25-0.30	17.344	
With polyamide covers	With electret washers	0.46-0.53	21.242	Very high
		0.25-0.30	22.182	
	Without	0.46-0.53	19.148	High
		0.25-030	19.0659	

As it could be seen in Fig. 2, Table 4 and 5 the working range of the current of electrification for disks charged by composition pastes is 45-165 nA and for disks charged by the castor oil it is of 30 - 105 nA.

Table 5. Dependence of the parameters of saw on electrophysical features of the process

Average value of ESCD on electret plates [C/cm²]	Intensity of electric field between plates [kV/cm]	Saw intensity Q [mm²/h]	Processing quality
$4 \cdot 10^{-4}$	400	22.330	Very high
$1 \cdot 10^{-4}$	100	22.218	"
$6 \cdot 10^{-5}$	60	21.984	"
$1 \cdot 10^{-5}$	10	21.013	"
$3 \cdot 10^{-6}$	3	19.215	High
No plates	0	19.153	"

Application of electret washers allows to increase the speed of saw by 9%, to abate noise by 5 dB, to decrease losses by 1%. The higher quality of saw lets decrease losses during the following operations, in particular during grinding, and short the duration of grinding. At the same time there is no necessity in special energy supply and the vibration resistance is better.

4. TECHNOLOGY OF POLYMER COVERS

On the base of established laws of the electrification of disperse polymers under dynamic forces a number of methods and constructions of the device of stationary type and in the form of sprayng gun were developed to realize the special tehnology of polymer covers.

In Fig. 3 there is a layout of the electrostatic set-up marked out by its autonomy due to no need in compressed gas and in special supply of high voltage. The set-up

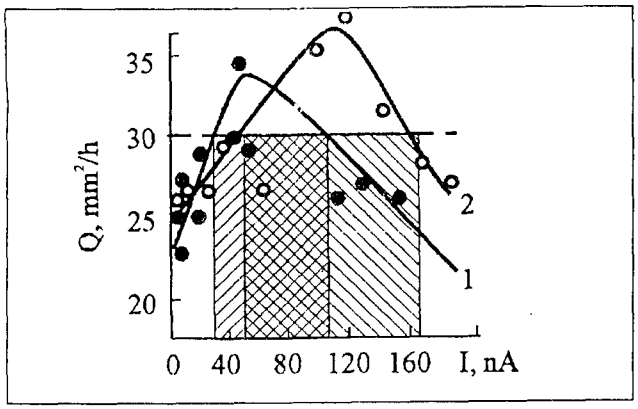

Fig. 2. Dependence of saw productivity versus the average current of electrification in the case of the sawing disks charged by different diamond content pastes: 1, serial paste; 2, composition paste. Shaded area corresponds to rational productivity.

includes the autonomic electrostatic generator using the closed circulation of air-powder mixture and the working reservoir 7 for cover spraying. The generator consists of the engine 10, scroll 1 with impeller 2, circulation tubes 3 and the collector 4. The high voltage from the collector carries through the conductor 5 to the charger 6. The unit 8 is grounded. A transmission of the rotation from the engine to the charger is carried out by a flexible shaft 9.

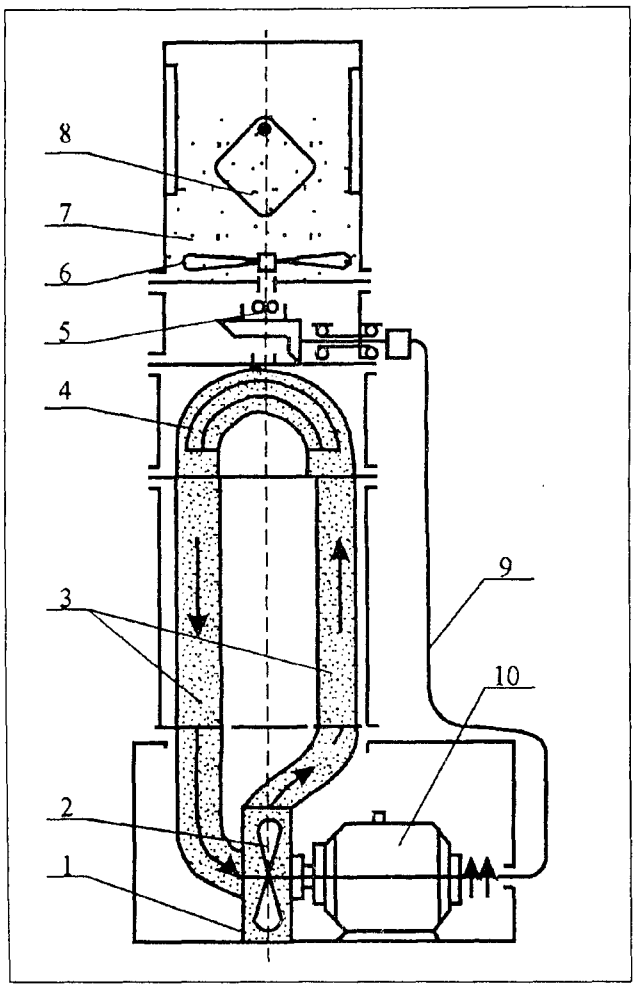

Fig. 3. The layout of the electrostatic set-up for polymer covering

The circulation of particles having the high velocity provides the high-voltage generation (up to 100 kV and more).

In devices for polymer covering like the spraying gun described in the work [1], the electrification of the polymer powder is a result of impact and dynamic contact of the powder particles with a surface of the charger unit. The main part of such devices is that charger unit (its special features of construction).

The most typical device of this type is shown in Fig. 4. The device consists of a body 1, having an intake conduit for an air-dispersion of polymer sprayed, with handle 2; coaxially arranged rotor electrodes 3, 4 with blades 5; guiding nozzle 6 enveloping the blades; mixer 7 with outlet 8 connected by hoses 9 with an air intake 10 and with a fluodizing chamber 11. There is a valve 12 on a hose connecting the mixer with the air intake. Also the spraying gun has a valve 13. The outer rotor electrode 3 is fixed in a support 14 and the inner one is fitted with clearance on an axis 15.

The device works in the following way. The disperse polymer is put into the fluodizing chamber 11. A compressed air or gas, initiated the fluodization [1] of the powder, is fed under porous partition of that chamber. The gas provides also feeding of the powder by hose 9 to the mixer 7 and then through the outlet into the working zone. Using the mixer one can extra feed an air from the air intake 10 by the valve 12.

The polymer gas-dispersion under the high pressure with high speed puts on the rotor electrodes. Here, after multiple and graduate connections and disconnections of the particles with the metal surface of electrodes, charges are generated on particles. In this case to obtain

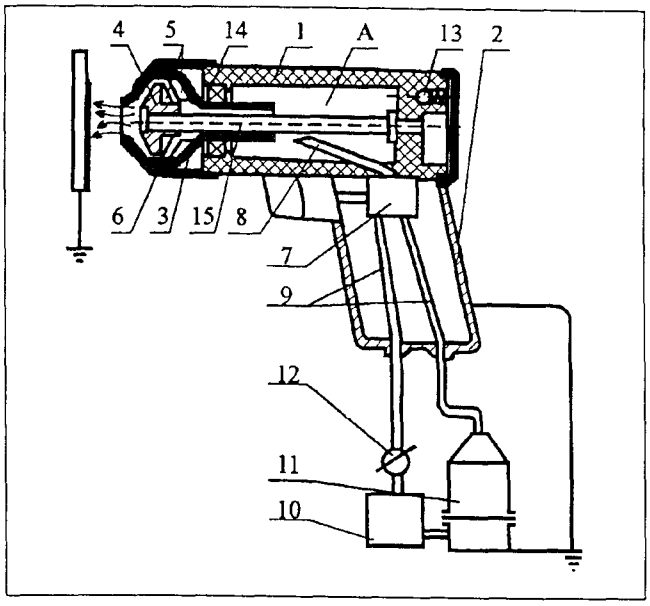

Fig. 4. The spraying gun for polymer covering. Spraying gun was developed to realize the special technology of polymer covers

great charges on the polymer particles the velocity of gas-dispersion at the exit to the inter-electrode space must be not less than 10 m/s.

By this device it is possible to cover with high productivity as cold surfaces with following fusion as previously heated. Also it is possible to cover items with a complex shape and as assembly units. The process is easy automated.

5. CONCLUSION

During last decades tribologists are studying and trying to explain numerous emission displays of the response of material surface layers to tribo-deformation effects. Among them the most informative are electron emission, electromagnetic radiation in the range from radio-frequencies to X-rays, different acoustic and low-frequency vibrations, but registration and explanation of them meet essential difficulties, which are a result of the following: those effects take place only during the frictional interaction; their results are hard to separate integral, morphology, and structure surface changes. Maybe the only universal and easy to identify "witness of macro- and micro dramas" taking place on friction surfaces is the electrification of surface.

The understanding of the triboelectrification mechanism had begun only after creation of quantum mechanical models in physics and chemistry of surface, ideas about electron energy levels, theory of molecular forces, based on conceptions of fluctuating electromagnetic fields of condensed media. Polymers are sensitive indicators of triboelectric phenomena. Investigations of polymers have allowed to essentially broaden knowledge on the structure mechanism of tribo-deformation and tribo-destruction of solids. The discovery of the triboelectret phenomenon as a result of the frictional electrification of polymers is very important. Establishment of the fact of the interconnection between tribo-electretization and triboelectrification has let develop the theory on friction and wear but also apply them in industries dealt with intensive frictional interactions and developing new tribo-technical materials.

REFERENCES

[1.] KLIMOVICH A., SVIRIDENOK A., **Electric phenomena at the polymer friction**, Minsk, "Nauka I tekhnika",1994, 268 p. (in Russian).

[2.] BAUSER H., **Dechema-Monographien**, Frankfurt am Main,1974, Bd, 72,11-29.

[3.] BILYAK SH.M., **Friction pair of metal-plastics in machines and devices**, Moscow, 1965, 245 p. (in Russian).

[4.] GODE M., **Simulation of friction and wear processes,** Friction and wear, 1991, V.13, No.1, 27-42 (in Russian).

[5.] POLYAKOV A. A., GARKUNOV D. N., **In coll. "Physical-and-chemical mechanics of contact interaction and fretting-corrosion"**, Kiev, 1973, 11-13 (in Russian).

[6.] MIRONOV V. S., POVZNER M. T., KLIMOVICH A. F., **In coll. "Current state and perspectives of progress of the diamond production"**, Smolensk,1981, 29-32 (in Russian).

[7.] MIRONOV V.S., BOCHAROV A. M., KLIMOVICH A.F., **Superhard materials**, 1985, Part 3, 61-64 (in Russian).

Primena triboelektričnih pojava u industriji

Za praktičnu primenu glavne triboelektrične pojave su elektrifikacija kontakta usled generisanja električnih napona i nastanak elektrisanog stanja u polimeru (elektret). Proučavajući kretanje visokih temperatura rasutih polimera na tribo- kontaktima, ustanovljen je domet elektrifikacije rasutih čestica (do 250 kV), kao i generisanje elektret stanja na njihovim površinama. Upravljajući, na primer triboelektričnim parametrima, i čineći elektret punioce delom kompozita, može se povećavati ili smanjivati elektromagnetsko polje generisano na tarnom kontaktu, to jest, može se realizovati elektret - triboelektificirani sastav.

Использование трибо-электрических явлений в промышленности

Среди всех трибологических явлений для использования на практике наиболее удобны "электрификация" контакта, являющаяся в результате генерирования электрических напряжений, и возникновение заряженного состояния в полимере. Исследованием развития высоких температур рассеянных полимеров в трущихсях контактах установлен уровень заряжения рассеянных частиц (до 250 кВ), как и развитие заряженного состояния на их поверхностях. Исследования показали. что управлением трибо-электрическими параметрами и использованием электрических наполнителей в качестве составляющих композита, можно увеличивать или уменьшать электромагнитное поле, формирующееся в контакте, т.е. можно создавать трибоэлектрифицированный состав.

UDK 621.9.015.004.6

V. G. BARSUKOV, V. YA. PRUSHAK,
V. YA. SHCHERBA, A. I. SVIRIDENOK

The Effect of Friction on The Extrusion of High-filled Composites

1. INTRODUCTION

Methods of screw and plunger extrusion are very extended at manufacture of profile articles made from different materials, but processing of high-filled composites by these methods is kept back due to insufficiently known factors like the effect of friction of the filler with itself as well as with working units of equipment on forming processes.

The following factors could be explained by tribology phenomena in rheology of high-filled composites: increasing viscosity in comparison with an initial polymer by some orders of magnitude; a display of features of solids for melts; considerable energy dissipation on surfaces of the contact between processing material and performing organs; a transition from laminar flow to rheologically more complex flows including plug sliding.

The aim of this investigation is to study the influence of friction forces on additional material heating in extrusion process, and on conditions of transition from viscous-plastic flow to the plug sliding flow in main profile channel types (circular, ring, rectangular, and rhombus).

2. FRICTIONAL MATERIAL HEATING

During friction forces action on the sliding surfaces of moulding material on the extrusion channel walls heat is being discharging. Specific power of this thermal energy q is equal multipli specific friction forces τ_0 by moulding material sliding velocity U in extrusion channel

$$q = \tau_0 \cdot V.$$

For generally used sliding velocities $V = 1 \div 2\ m/min$ and specific friction forces $\tau_o = 0.2 \div 0.4\ MPa$ energy dissipation will be value of order $q = 3.3 \div 13.5\ kW/m^2$, that is comparable with power thermal flow from other thermal heaters. The experiments showed that additional material heating from friction force action may exceed $30 \div 50^oC$. For composites with low thermal stability this assumes to apply special means (introduction to composite technological lubrications, thermo-stabilizers, forced heat diversion from frictional surfaces).

3. TRANSITION FROM VISCOUS-PLASTIC FLOW TO PLUG-SLIDING

From points of view of physics and mechanics the process of extrusion plug sliding regime may occur when next two conditions are fulfilled:

a) flow nucleus is spreading to the full cross-section of extrusion channel;
b) composition adhesion to the channel walls is replaced with its sliding on this walls.

It follows from the first condition that specific friction forces of composition on the channel walls and tangential stress in its bulk must be lower than composition shear strength, i.e. unreversible material deformation in plug sliding zone is absent, and deformation has elastic or viscous-elastic nature.

Accounting short time of material being in plug sliding zone, and also that viscous-elastic behavior may be des-

Vladimir G. Barsukov, Anatoly I. Sviridenok
Research Center on Resource Saving of Belarus Academy of Sciences, Grodno, Belarus
Victor Ya. Prushak, Vladimir Ya. Shcherba,
Soligorsk Institute on Problems of Resource Saving, Soligorsk, Belarus

cribed, with precision sufficient for practice, by elasticity equations, in which elastic constants are replaced with viscous-elastics operators [1]; the consideration of stress-deformed condition of material in plug sliding zone is restricted to the elastic approach.

The condition of transformation from plug sliding to viscous-elastic flow is considered in the form of energetic yield criterion.

Taking under the consideration boundary condition on the surfaces of composition contact with extrusion channel walls we originate from Amontons-Coulomb friction law that is correct only for low pressure field, when actual contact area of bodies is smaller than nominal area. At high pressures the saturation of contact surfaces occurs and friction force became undependent of pressure [2,3]. In a connection with it, for description of frictional phenomena in plug sliding zone, the friction law in Zibel-Prandtl form is used [2].

In calculations the compositions have shear strength τ_S, elasticity modulus E and Poison's coefficient ν, at pressures lower than flow beginning. Specific friction forces on the channel walls are equal to τ_O.

Base on the developed approach a number of theoretical tasks, which have important practical meaning for calculation of extrusion devices and technological equipment, have been solved.

Circular channel. Composition plug sliding in a circular channel of radius R is characterized by next parameters:

a) distribution of axial p and lateral q pressures on the length of plug sliding zone

b) length of plug sliding zone

$$p = \frac{2\tau_0}{R} x,$$

$$q = \frac{2\tau_0}{R} \cdot \frac{\nu}{1-\nu} x;$$

c) limit value of specific friction forces $[\tau_O]$, which ex-

$$L = R \frac{1-\nu}{1-2\nu} \sqrt{\left(\frac{\tau_S}{\tau_0}\right)^2 - \frac{3}{4}};$$

ceeding led to propagation of viscous-elastic flow regime to the whole length of extrusion channel

Channel of rectangular cross-section. Such channels are

$$[\tau_0] = \frac{2}{\sqrt{3}} \tau_S$$

used for extrusion of stripes, sheets, beams and other similar profiles.

Composition plug sliding in the rectangular cross-section channel with height H and width B is characterized with next parameters:

a) distribution of axial p and lateral q pressures on the length of plug sliding zone

$$p = 2\tau_0 \frac{B+H}{BH} x,$$

$$q = 2\tau_0 \frac{\nu}{1-\nu} \frac{B+H}{BH} x;$$

b) length of plug sliding zone

$$L = \frac{1-\nu}{1-2\nu} \frac{BH}{B+H} \sqrt{\left(\frac{\tau_S}{\tau_0}\right)^2 - \frac{3}{2}};$$

c) limit value of specific friction forces

$$[\tau_0] = \sqrt{\frac{2}{3}} \tau_S.$$

Channel of rhombus cross-section. The solution of this problem was directed to investigation of product forming peculiarities with acute vertex. The regime of composition plug sliding in the rhombus cross-section channel with side length C and acute angle α at vertex has next parameters:

$$p = \frac{4\tau_0}{C \sin\alpha} x,$$

$$q = \frac{\nu}{1-\nu} \frac{4\tau_0}{C \sin\alpha} x$$

$$L = \frac{1}{2} \frac{1-\nu}{1-2\nu} C \cos\frac{\alpha}{2} \sqrt{\left(\frac{\tau_S}{\tau_0} \cdot 2\sin\frac{\alpha}{2}\right)^2 - 3},$$

$$[\tau_0] = \tau_S \cdot \frac{2}{\sqrt{3}} \sin\frac{\alpha}{2}.$$

From the obtained formula one can see that decrease of angle at vertex led to worsen of processing conditions, since axial and shear pressure rapid increases simultaneously with limit values of specific friction force.

Ring channel. This channel ise used in pipe and hose production. Plug sliding regime in such channel with outer radius R_O and inner R_I will be characterized with next parameters:

$$p = \frac{2\tau_0}{R_O - R_I} x,$$

$$q = \frac{2\tau_0}{R_O - R_I} \frac{\nu}{1-\nu} x,$$

$$L = (R_O - R_I)\frac{1-\nu}{1-2\nu}\sqrt{\left(\frac{\tau_S}{\tau_0}\right)^2 - \frac{3}{4}};$$

$$[\tau_0] = \sqrt{\frac{2}{3}}\tau_S.$$

The presented data together with earlier published results on cracks forming [4] or distortion of non-axis-symmetrical profile [5] at friction force action allow to account frictional aspects of extrusion processes of high-filled composites in the group and to control goal-directed them.

REFERENCES

[1.] RABOTNOV YU. N., **Mechanics of deformed solids**, Moscow, Nauka,1979 (in Russian).

[2.] DRUYANOV B. A., **Applied theory of porous solids plasticity**, Moscow, Mashinostroenie,1989 (in Russian).

[3.] MAKUSHOK E. M., KALINOVSKAYA T. V., BELY A. V, **Mass-transfer in friction processes**, Minsk, Nauka i tekhnika,1978 (in Russian).

[4.] BARSUKOV V. G., KUPCHINOV B. I., LAPSHINA E. M., **Strecht strain in extrusion profiles form high-filled moulding materials**, Vestsi Akademii Nauk Belarusi. Phys.-tekh. Part.1994, N°1, p.11-14 (in Russian).

[5.] BARSUKOV V. G., KUPCHINOV B. I., ANTONOV V. P., **Plug sliding zone parameters in extrusion of non-axial symmetric wood-plastic products**, Vestsi Akademii Nauk Belarusi. Phys.-tekh. Part. 1993, N°4, p.20-23 (in Russian).

Uticaj trenja na istiskivanje visoko - punjenih kompozita

Analiziran je uticaj sila trenja na zagrevanje visoko - punjenih kompozita u procesima istiskivanja. Razmatrane su reološke specifičnosti tečenja i klizanja materijala koji se oblikuje u alatima za formiranje kanala opreme za istiskivanje.

Влияние процесса трения на выдавливание высокозаполненных композитов

В работе анализируется воздействие сил трения на нагревание высокозаполненных композитов в процессах выдавливания. Рассмотрены также и реологические особенности течения и скольжения материала по канавкам пресс-форм.

ISTRAŽIVANJA

UDK 621.892:621.9.027

N. N. ANTONESCU, A. C. DRUMEANU, I. NAE

Wear by Thermal Fatigue and Steels Durability from Mechanical Brakes Dry Friction Couplers

1. INTRODUCTION

Thermal fatigue phenomenon generally appears in metallic structures submitted to variable thermal stresses. Following these stresses, thermal stress appears, which have high values that can sometimes go beyond the metallic materials yield limits.

A specific field to show this phenomenon is the dry friction couplers from the mechanical brake assembly. Indifferently of the construction solution adopted for making such a mechanical brake system, the operating principle is based on the friction existence between two elements, from which at least one is generally metallic. In these conditions, the metallic materials support almost entirely the thermal stress, generally generated in the stratum adjacent to the friction surface.

The paper wants to present the results of the experimental studies concerning the complex phenomenon of the thermal fatigue wearing of some low and middle alloy steels used in drums from mechanical band brakes construction of the drawworks.

The maximum temperature on the friction surface of the brake drum can reach values in the range of 500 ... 800°C [1]. In these conditions, the drums decay occurs by cracking and has a character similar to that characteristic to low cycle fatigue.

N. N. Antonescu, A. C. Drumeanu, I. Nae
"Oil-Gas" University Ploiesti

2. CHEMICAL COMPOSITION AND MECHANICAL CHARACTERISTICS OF THE STUDIED STEELS

The studied steels were the following:

1) low alloy steel put into pieces T35Mnl4 (steel 1);
2) middle alloy steel put into pieces T32MoCrNiO8 (steel 2);
3) low alloy steel 35Mn14 (steel 3);
4) alloy steel 40BCr10 (steel 4).

Chemical composition and mechanical characteristics of these steels are presented in Table 1 and Table 2.

Table 1. Chemical composition of the steels.

Chemical alloying elements	Steel			
	1	2	3	4
	Composition [%]			
C	0.35	0.32	0.35	0.40
Mn	1.40	0.81	1.40	0.65
Cr	0.30	0.74	-	1.00
Ni	0.30	0.60	-	-
Cu	0.30	0.26	-	-
Si	0.24	0.23	0.27	-
Mo	-	0.18	-	-
B	-	-	-	0.002

These steels were selected to be studied because they were generally used for the construction of the friction metallic elements of the dry friction couplers from the mechanical brakes.

Table 2. Mechanical characteristics of the steels.

Mechanical characteristic	Steel			
	1	2	3	4
Tensile strength [MPa]	540	740	720	930
Yield limit [MPa]	295	540	530	735
Elongation [%]	12	15	16	12
Reduction of area [%]	25	25	30	50
Hardness HB	160	220	200	217

3. THEORETICAL CONSIDERATIONS ABOUT THE DURABILITY TO THERMAL FATIGUE OF THE METALLIC MATERIALS

The degradation of the metallic materials used for mechanical brakes construction generally consists of cracks appearance after a low number of braking cycles.

In these conditions, the gradual process of degradations accumulation occurs in the presence of plastic preponderent strains, materials crash taking place due to the cyclic strains, the compression strain which appears at the thermal cycle, having the major role.

The basic principle in the elaboration of the model of the thermo-mechanical behaviour analysis of the materials to thermal fatigue, implies the sample fastening during its heating (by clamping it at both ends) and it was elaborated by Coffin. The characteristic parameters of this theoretical model can be put into a relation like:

$$\Delta\varepsilon = \alpha(t_{max} - t_{min}) = \Delta\varepsilon_e + \Delta\varepsilon_p = \frac{\Delta\sigma}{E} + \Delta\varepsilon_p \qquad (1)$$

where: $\Delta\varepsilon$ - the total strain range;
$\Delta\varepsilon_e$ - elastic strain range;
$\Delta\varepsilon_p$ - plastic strain range;
α - linear thermal extension of the material;
E - modulus of elasticity longitudinal at the average temperature of the stress-strain hysteresis loop (Fig.1);
$\Delta\sigma$ - range of stress.

In real situations of temperature variation, generally, it is determined the strain range in a cycle, which doesn't depend essentially of the mechanical properties variations of the material. The strain is determined with the help of the linear thermal coefficient of expansion of the material and with the difference of temperature (t_{max}-t_{min}). The maximum value of the plastic strain range on the cycle, unlike the total strain range, depends on the mechanical characteristics of the material, influenced by the cyclic stress and by the structure preservation between the cyclic heatings, that means all the factors that influence the stress-strain hysteresis loop (Fig.1).

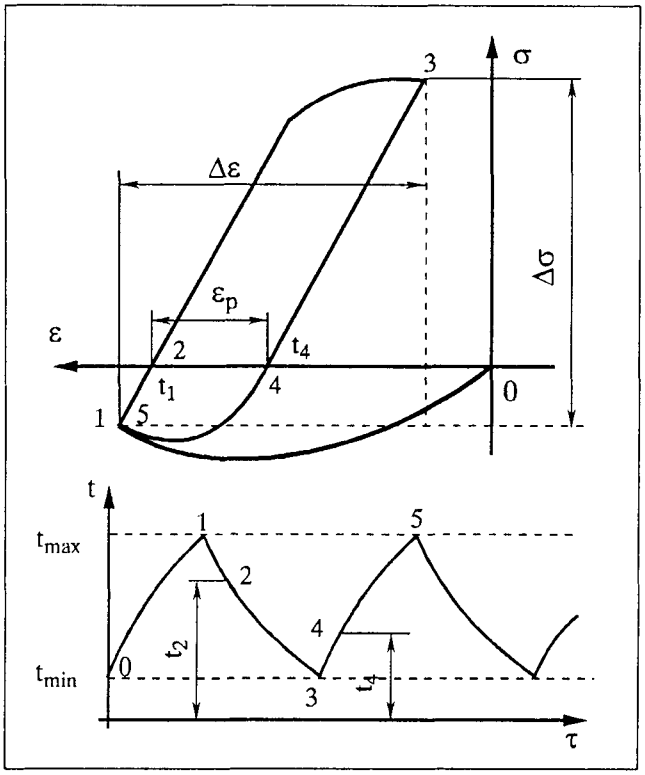

Fig.1. The stress-strain hysteresis loop

The thermal fatigue endurance limit is given by many complex characteristics of the material (mechanical, physico-chemical, structure), and by the character of the external loading.

In most of the situations, thermal fatigue endurance limit is evaluated using a durability criterion, which consists of the number of cycles, N, determined till the first crack appearance or until deformation capacity decrease to the same maximum temperature under a certain limit.

The results obtained, generally respect the experimental curves of thermal fatigue $N=f(\Delta\varepsilon)$ or $N=f(\Delta\varepsilon_p)$, and they are in accordance with the calculated values of the constants adopted for the durability equations Manson-Coffin like, [2, 3]:

$$\Delta\varepsilon_p \cdot N^{k_1} = C_1 \qquad (2)$$

$$\Delta\varepsilon \cdot N^{k} = C \qquad (3)$$

where: N is the number of cycles until the first crack appearance;
$\Delta\varepsilon_p$ - plastic strain range [%];
$\Delta\varepsilon$ - total strain range [%];
k_1, k - exponents of durability;
C_1, C - durability constants characteristic to each material.

About equations (2) and (3) utilization the following remarks can be made:

- at total strain range values lower than these corresponding to the same stress that exceeds the yield limit, the number of the cycles until degradation, calculated with the relation (2), should be theoreti-

cally unlimited, as far as the plastic strain tends to zero, which is not in accordance with the experimental data;

- the determination of the highest value of the plastic strain with the relation (3) would be inaccurate, as a result of the difficulty in material hardening evaluation (Bauschinger effect) and of stress relaxation phenomenon;
- Manson - Coffin equation does not take into consideration the maximum temperature of the cycle maintenance.

4. THE EXPERIMENTAL TESTING METHODOLOGY

The experimental determinations were done on cylindrical filled samples with the following characteristics:

- total length - 70 mm;
- calibrated zone length - 30 mm;
- calibrated zone diameter - 4 mm;
- threaded gripping heads - M10;
- thread length -15 mm.

The samples were electric heated, current thermal effect being concentrated in the minimum section zone, where maximum temperature was reached.

For determinations it was used a thermal fatigue testing stand, which assured enclosure fastening at both ends of the sample in a rigid frame. The fastening system rigidity can be modified depending on the maximum level of the total elastoplastic strain to which the sample is cyclically strained (tested to compression stress at the maximum temperature of the cycle, and to tensile stress at the minimum temperature of the cycle).

Started from the real data from the brake drums running [1], the testing experimental conditions of the samples were:

- maximum temperature of the cycle, $t_{max} = 800^oC$;
- minimum temperature of the cycle, $t_{min} = 100^oC$;
- heating time, $\tau_h = 8 ... 12$ *seconds;*
- cooling time, $\tau_c = 90 ... 120$ *seconds;*
- time of the exposure to maximum temperature of the cycle, $\tau_e = 0$ *seconds* (periods of time are similar to that registred in reality).

The experiments were done using three steps of rigidity of the sample enclosure frame: 12, 28, 55 MN/m, which gave the possibility to obtain the same total elastoplastics strains in the range of 0.3 ... 1.2%, corresponding to some levels of the stress, $\Delta\sigma$, in the range of *150 ... 900 MPa,* similar to those experimentally and theoretically determined [4]. The tests were done at a constant strain range and the stopping criterion was the first crack appearance. The total strain range of the frame and hence also of the sample, was measured with the help of two dial extensometers, with 0.01 mm accuracy. The stresses from the sample were calculated knowing the force with which, after dilatation, it strains the calibrated elastic element which is the upper part of the frame that regulates its rigidity.

5. EXPERIMENTAL DETERMINATIONS OF THERMAL FATIGUE DURABILITY

The experimental determinations were done according to the methodology described in section 4, using the experimental parameters presented in Table 3.

During the whole period of the experiment, there were registered:

- the value of the total strain range of the sample;
- the number of the cycles until the first crack appearance;
- stress range per strain cycle.

In accordance with the experimental data, the durability curve was plotted, in $\Delta\varepsilon(\%)$ - N(cycles) coordinates, represented in double logarithmic scale in Fig.2.

Starting from the equation (3) a relation can be written N - $\Delta\varepsilon$ which takes care of the total duration of the thermocycles, like:

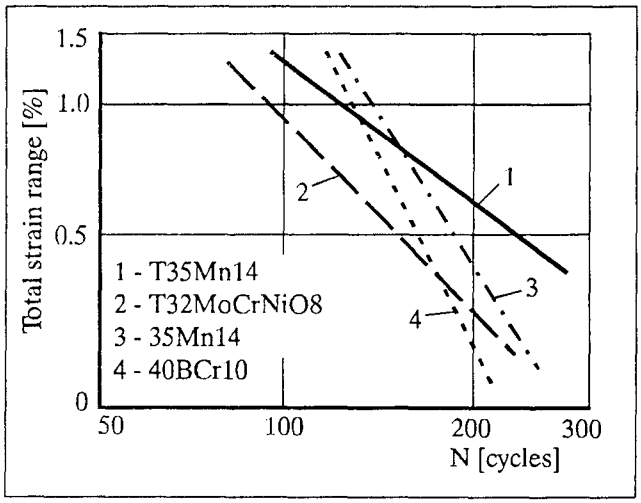

Fig. 2. The total strain range versus the number of cycles until degradation appearance

Table 3. Experimental parameters used for thermal fatigue durability determinations.

Experimental parameters	Steel			
	1	2	3	4
Maximum temperature of the cycle [°C]	800	800	800	800
Minimum temperature of the cycle [°C]	100	100	100	100
Heating time [s]	12	10	10	9

Cooling time[°C]	115	106	120	108
Time of exposure [s]	0	0	0	0

$$N = \frac{1}{(4 \cdot \tau_{cicle})^b} \cdot \left(\frac{C}{\Delta\varepsilon}\right)^{\frac{1}{k}} \qquad (4)$$

where: N is the number of the cycles until the first crack appearance;
τ_{cycle} - thermal stress cycle duration;
$\Delta\varepsilon$ - total strain range per cycle;
C, k, b - experimentaly determined material constants, that can be found in Table 4.

Table 4. Material constants values from Eqs. (3),(4), (5) for the studied steels

Constants	Steel			
	1	2	3	4
k	1.357	1.58	1.86	1.505
C	662.9	1218.7	1850	1215
b	1.52-1.6	1.34-1.45	1.2...1.75	1.45...1.59
p	2.6	2.93	3.71	1.42
C_2	1082.2	994.8	2462.7	327.8

The influence of the total duration of the cycle on the durability can be made evident independently of the Mason - Coffin equation coefficients, using the relations:

$$(\tau_{cycle})^p \cdot N = C_2 \qquad (5)$$

$$(\tau_{cycle})^{p-1} \cdot N = C_2 \qquad (6)$$

where: τ_{cycle} is the mean duration of a thermal stress cycle;
N - the number of the cycles taken into consideration;
p, C_2 - material constants calculated for $t_{max} = 800°C$ in Table 4.
R - durability resource (until degradation appearance).

$$R = \tau_{cycle} \cdot N \; [min] \qquad (7)$$

Equation (5) plotting in double logarithmic coordinates, (Fig. 3) is linear and in good agreement with the experimental results [2,3] for values of the thermal stress cycle duration, $\tau_{cycle} = 1.3 \ldots 120$ *min.*

The durability resource is also influenced by the total strain range value, $\Delta\varepsilon$. This phenomenon was made obvious in Fig. 4.

The fact must be mentioned that Eqs. (5) and (6) can not be used for the durability calculations for different metallic materials, but they can be used in comparative estimations.

An estimation, as objective as possible, of the materials behaviour tested to thermal fatigue, only on the basis of the curves like that presented Fig. 2, would be incorrect if it were made only by analogy with the tests to low cycle isothermal fatigue, to which the total strain range is imposed. Specific for the thermal fatigue tests is their

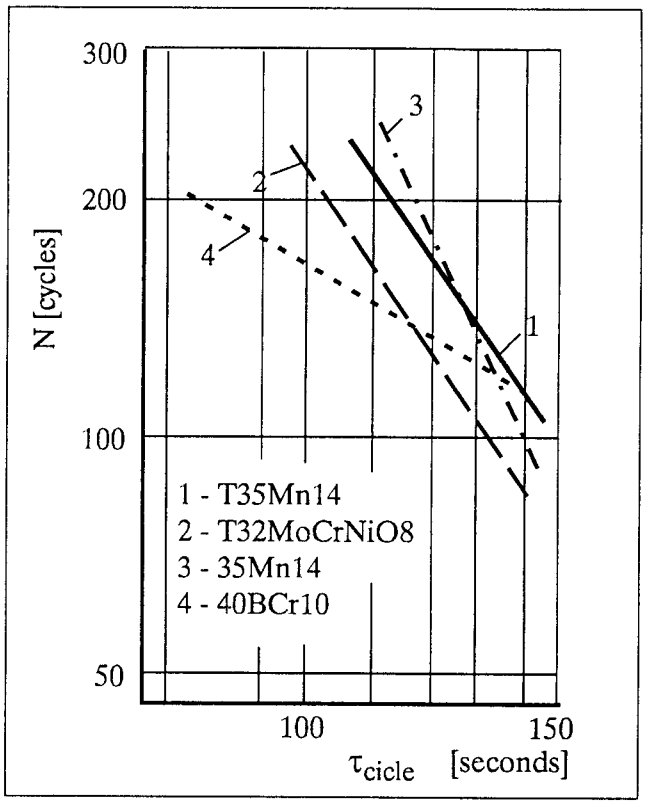

Fig. 3. The number of cycles until degradation appearance versus the mean duration of a thermal stress cycle

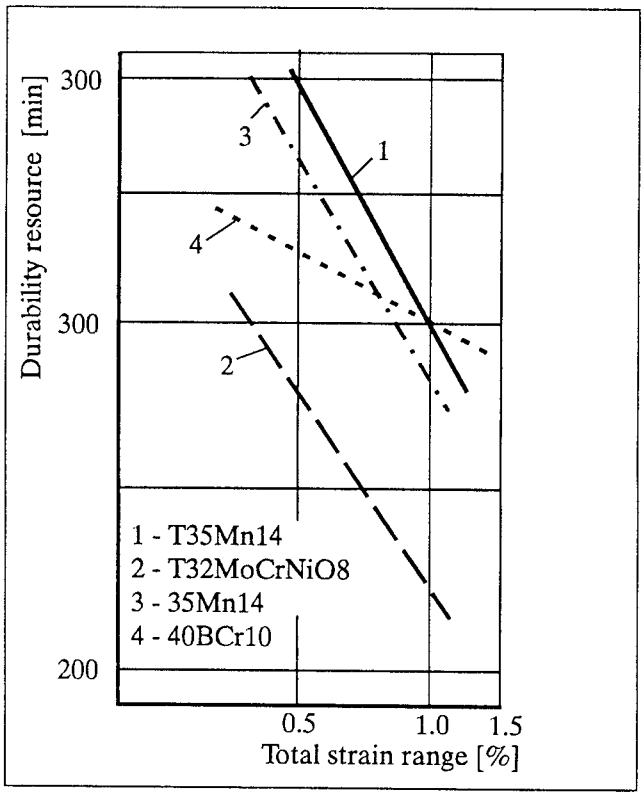

Fig. 4. The durability resource versus the total strain range

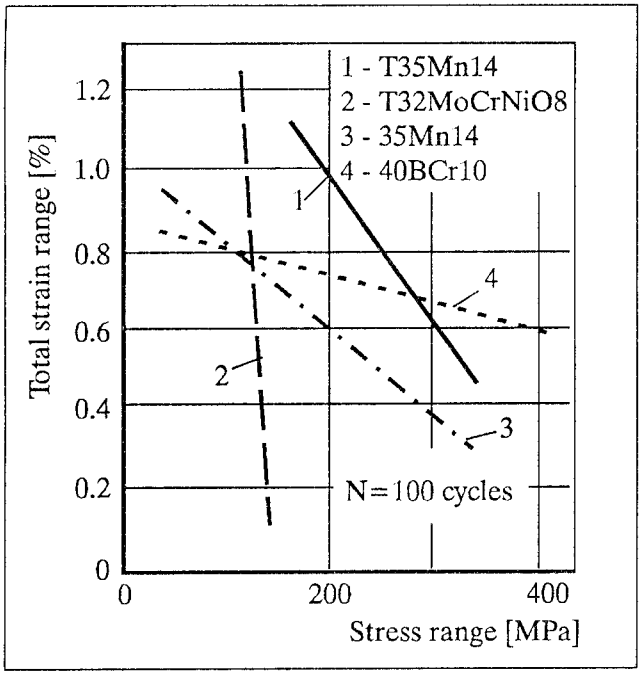

Fig. 5. The total strain range versus the stress range (for N =100 cycles)

development at constant maximum temperature of the cycle. In this case the interpretations regarding the hardening phenomena have specific aspects.

So, for the studied steels there were observed the following things:

- under the conditions in which the thermal total strain range ($\Delta\varepsilon$) is done only by the temperature variation between two constant limits, hysteresis loop stabilization occurs, usually, till values of $N \leq (60...70)$ *cycles*, when stress range ($\Delta\sigma$) becomes approximately constant;
- taking into account the fact that the tests are done with an imposed total strain range, the hardening of the tested steels progresses until it reaches the saturated hardening state, as is was specified before;
- the stress range ($\Delta\sigma$) reduction is in accordance with the number of cycles characteristic for degradation (appearance of the crack) and is explained by deformation capacity reduction of the material, due to the crack appearance and propagation;
- the influence of the system rigidity in which the sample was done and though of the stress range, at a certain number of cycles, on the total strain range is well evidenced in Fig. 5, where it can be observed that the alloy steel 40BCr10 has the best behaviour for $N=100$ strain cycles and average values of the total strain range ($\Delta\varepsilon \approx 0.6\%$), while the middle alloy steel T32MoCrNiO8, at the same value of the range of stress has the highest possible of deformation ($\Delta\varepsilon \approx 1.0\%$).

6. CONCLUSIONS

Analyzing the results of the experimental determinations concerning the behaviour of the metallic materials used for the dry friction couplers construction from the mechanical brakes to thermocyclic strains we can draw the following conclusions:

- the main cause of the degradation by cracking, of the metallic elements of the mechanical brakes are the thermal stresses generated by the nonuniform heatings which appear during the brake processes;
- the durability curves to thermal fatigue, experimentally determined, show the behaviour for different stress conditions; so, the alloy steel 40BCr10 has a better durability at high values of the strain than the other steels;
- in the presented testing conditions, the relativelly fast reaching of the saturated hardening state diminishes very much the structures durability and favours cracks initiation and propagation;
- the durability curves from Fig. 2 can be used in design calculations as far as there can be determined the maximum elastoplastic strains of the thermocyclic stressed metallic structures;
- the duration of the thermal cycle influences the durability in the way of its lowering simultaneously with the increase of the heating-cooling time;
- alloying elements influence, especially for high values of the total strain, is favourable in the case of the steels alloyed with Mo, Cr, Ni;
- the results obtained after the simulation of the heating-cooling cycles from the brake couplers on samples are in good agreement (from the order of magnitude point of view) with the real durability, practically observed, of the metallic structures from these couplers.

REFERENCES

[1.] SAHMALIEV, G. M., TAGIEV, S. M. AND RODJABOV, S. A., **Opredelenie temperaturi poverhnosti trenia mehaniceskogo tormoza pri ego sovmestnoi rabote s gidrotormozom**, Masini i neftianoe oborudovanie, 5, 1967, 14-18

[2.] DULNEV, R. A., KOTOV, P. I., **Termiceskaia ustalost metallov**, Moskva, Masinostroenie, 1980

[3.] TULIAKOV, G. A., **Termiceskaia ustalost v teploenerghetike**, Moskva, Masinostroenie, 1978

[4.] FARADJEV, T. G., GUSEPOV, I. B., ALIEV, A. M., ALIHANOV, N. R., **Issledovanie nestationarnnoi temperaturi i temperaturnih napriajenij frictionnoi pari tormoza burovoj lebedki**, Nefti i Gaz, 2, 1977, 91- 95

ISTRAŽIVANJA

UDK 621.833.044.6

I. BERCEA, N. MITU, I. DAMIAN, M. BERCEA, S. CRETU

A Theoretical and Experimental Study on Friction Losses in a Tapered Roller Bearing

1. INTRODUCTION

The friction torque is the most common parameter used to appreciate frictional losses in a rolling bearing. Based on experimental investigations various equations have been reported in literature to evaluate the friction torque of tapered roller bearings that work at low loads and rather moderate speeds, [1, 2]. In the high speeds domain these simpler equations are not longer valid, all sources of friction losses have to be carefully evaluated.

To estimate the friction torque for the particular case of tapered roller bearings running at high speeds, under combined loads some dynamic models have been presented in literature, but which separately consider the mechanical losses and tribological losses. To evaluate the friction coefficients, Gupta [4] considers the lubricant as a Newtonian fluid, while Zhou [3] uses the Maxwell-Ree-Eyring model with visco-elastic nature. On the other hand, Raczynski [5] and Wang [6] use the values of the friction coefficients as a function of the contact pressure and the sliding speed. Only, Gupta, [4] and Hams [7] take into account the frictions between the rollers and the cage with the air-lubricant mixture.

Recently, a complex model has been elaborated by authors, [8, 9], which incorporates all friction sources that were differenly used by previously dynamic studies [3, 7]. The experimental studies regarding the evolution of the friction torque at low speeds, imposed to supplement the model developed in [8], to consider the micro-asperity traction that is achieved in line contacts between tapered rollers and raceway.

Bercea Ioan, Mitu Nicolae, Damian Ioan, Bercea Mihai, Cretu Spiridon, Ph.D.
Technical University "Gheorghe Asachi" Iasi, ROMANIA

2. TORQUE PREDICTION MODEL

The main friction sources in a tapered roller bearing are:

(i) the viscous friction in lubricant film;
(ii) the rolling resistance of tapered rollers;
(iii) the microasperity tractions;
(iv) the hydrodynamic resistance;
(v) the spin friction;
(vi) the roller and cage resistance in the air-lubricant mixture.

The friction forces and the friction torques that act on tapered rollers, raceways, as well as, on the inner ring shoulder are evaluated using the methodology previously developed and presented in [8]. For each particular contact tribosystem the friction forces and torques are pointed out in Figure 1.

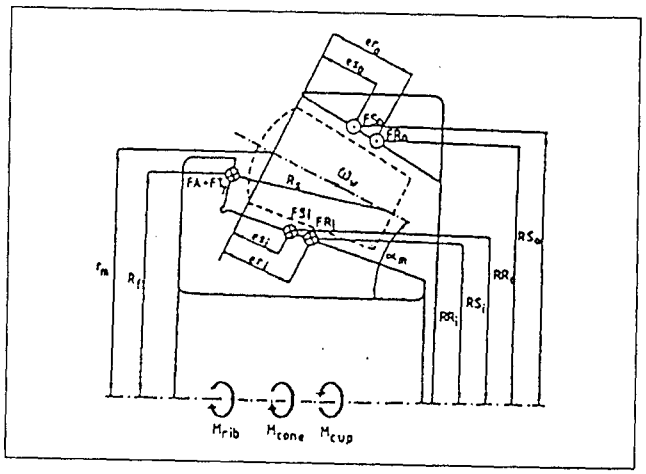

Fig.1. Forces and torques acting in a tapered roller bearing.

The friction forces *(FP)* determine the roller tendency to e translation motion and ere evaluated as in [10]. The equation proposed in [3], with a thermal correction, are used to calculate of rolling resistance forces *(FR)*. The sliding traction forces *(FS)* from line contacts and those from the elliptic point contacts, (Ft_y) ere determined by en integration operation applied to tangential stresses (τ) which are computed with the Maxwell-Ree-Eyring model, [11]. The traction forces developed on the micro-asperity contacts, *(FA)* are determined by using the results presented in [3].

The well known Dowson & Hamrock [12] film thickness formulae are used for both point and line contacts.

For each contact tribosystem an individual estimation of the friction torque were carried out:

(a) The bearing torque derived from Inner Raceway Contacts:

$$M_{cup} = M_i = \sum_{j=1}^{z} FS_{ij} \cdot RS_{ij} + \sum_{j=1}^{z} FR_{ij} \cdot RR_{ij} + \sum_{j=1}^{z} FA_{ij} \cdot RA_{ij}$$

(b) The bearing torque derived from Outer Raceway Contacts:

$$M_{cone} = M_o = \sum_{j=1}^{z} FS_{oj} \cdot RS_{oj} + \sum_{j=1}^{z} FR_{oj} \cdot RR_{oj} + \sum_{j=1}^{z} FA_{oj} \cdot RA_{oj}$$

(c) The bearing torque derived from the Rib- Roller End Contact:

$$M_{rib} = M_f = \sum_{j=1}^{z} \left(FT_{yf} + FA_f \right)_j \cdot R_f$$

Excepting for the particular case of the pure thrust loading, the radia *RS, RR, RA* and *RF* of tangential forces have individual values for each tapered roller.

Though the bearing friction torque is easier to be experimentally verified; the power friction loss represents the most adequate parameter to be optimized.

3. POWER LOSS PREDICTION MODEL

(a) Power Loss from Raceways Contacts

The power loss on both inner and outer raceways were determined as:

$$P_{kj} = \iint_{A_k} \Delta P_{kj} \cdot dydz + FA_{kj} \cdot \left(\bar{U}_{sy} \right)_k$$

where: ΔP_{kj} is the friction power developed on an elementary friction area, $\Delta y\ \Delta z$;

$$\Delta P_{kj} = \left(\tau_y \cdot \Delta y \cdot \Delta z \cdot U_{sy} \right)_{kj} \qquad k = i,\ o$$

U_{sy} represents the sliding velocity in the middle of the elementary area and $\bar{U}_{sy}$ is the sliding velocity in the area where the normal contact load Q_k $(k = i,\ o)$ is applied. It is estimated that in the same point the resultant traction force *(FA)* is also acting. The power loss on the entire raceway is:

$$P_{con,cup} = P_k = \sum_{j=1}^{z} P_{kj} \qquad (k = i,\ o)$$

(b) Power Loss from Rib - Roller End Contact

$$P_{fj} = \iint_{A_f} \Delta P_{fj} \cdot dy_f\, dz_f +$$

$$+ \left[\iint_{A_f} \left(\tau_{yf} \cdot z_f - \tau_{zf} \cdot y_f \right) dy_f\, dz_f \left(\Omega_W \right)_{xf} + FA_{fj} \cdot \left(U_s(0,0) \right)_k \right]$$

where ΔP_{fj} represents the power loss on an elementary area $\Delta y_f \Delta z_f$ of the contact ellipse.

$$\Delta P_{fj} = \tau_{yf} \cdot \left[U_s(y_f, z_f) \right]_{yf}$$

The power loss at the guiding shoulder contact is:

$$P_{rib} = P_f = \sum_{j=1}^{z} P_{fj}$$

(c) Power Loss from Roller - Cage Contact

$$P_{cj} = \mu_{cj} \cdot FC_j \cdot U_{sc}$$

where: μ_{cj} is the friction coefficient at roller- cage contact; *FC* is the normal contact load; U_{sc} is the sliding velocity at this contact.

For all cage's holes, the power loss is

$$P_{cage} = P_c = \sum_{j=1}^{z} P_{cj}$$

(d) Power Loss for Roller and Cage Churning

- roller churning:

$$P_{rd} = \sum_{j=1}^{z} FD \cdot U_W + \sum_{j=1}^{z} MD \cdot \Omega_W$$

- cage churning:

$$P_{cd} = MC \cdot \Omega_C$$

and the sum:

$$P_{oil\ churning} = P_{rd} + P_{cd}$$

where: *PD* represents the friction force realized by the roller advance in the air-lubricant mixture; *MD* is the resistance torque to roller rotation in air-lubricant mixture; *MC* is the cage friction torque in the air - lubricant mixture; U_W is the roller transport velocity in the air-lubricant mixture. The values for *PD, MD* and *MC* are evaluated with the equations proposed in [8].

(e) Total Power Loss

$$P_T = P_i + P_o + P_f + P_c + P_{rd} + P_{cd}$$

4. RESULTS AND DISCUSSION

Using the methodology developed in [8], the dynamic equilibrium was firstly performed. The values of the rotation speeds Ω_{wj} $(j=1, z)$ and Ω_c resulted from the dynamic equilibrium have been further used to evaluate the sliding velocities in each contact.

The analytical, as well as, experimental studies, were applied on a 30206 tapered roller bearing. A mineral oil was used as lubricant with the kinematics viscosity $\nu = 42\ cSt/50°C$ and $\nu = 7\ cSt/100°C$ and the density $\rho = 895\ kg/m^3$ at $20°C$.

The experimental rig is presented in Figures 2 and 3.

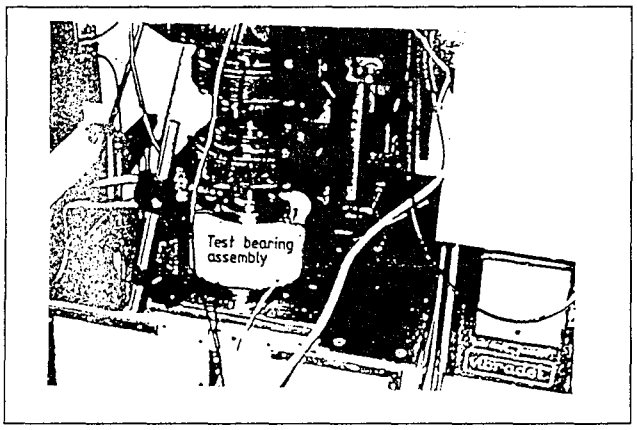

Fig. 2. General view of the measuring rig

The first testing bearing, *a*, is receiving the rotation motion from the main shaft through the cone *10*. The second testing bearing, *b*, is moved by the bearing *a* through the bushes *3* and *4* and the intermediate shaft *6*. The rotation of the case *6* is stopped by the pin *11* and the elastic beam *12* that has two electric resistance transducers, *13*, mounted on each face. During the running process the pin *11* acts on the elastic beam *12* with a load

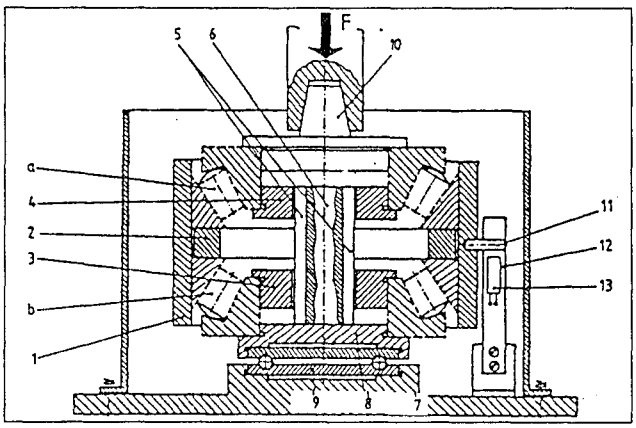

Fig. 3. Axial section through measuring device

proportional to the value of the friction torque achieved on the outer rings of the tapered roller bearings *a* and *b*.

The dependence of the friction torque, measured on the outer ring of the 30206 tapered roller bearing, with both rotation speed and axial load is given in Figure 4. For the same conditions in Figure 5 are presented the evolutions of the electrical resistance, the film thickness and of the lubrication parameter λ.

When the rotation speed is sufficiently low ($\leq 900\ rpm$) the dependence between the friction torque and the rotation speed is very similar to the well known Stribeck's curve from journal bearings.

The Figure 5 points out that for rotation speeds lower than 500 rpm a mixt lubrication regime is achieved, (1:5), so that the microasperity traction becomes more and more important, leading to increased values for the bearing friction torque. A quite good correlation is achieved between the experimental and theoretical values of the bearing friction torque, that proves the validity of the proposed analytical model.

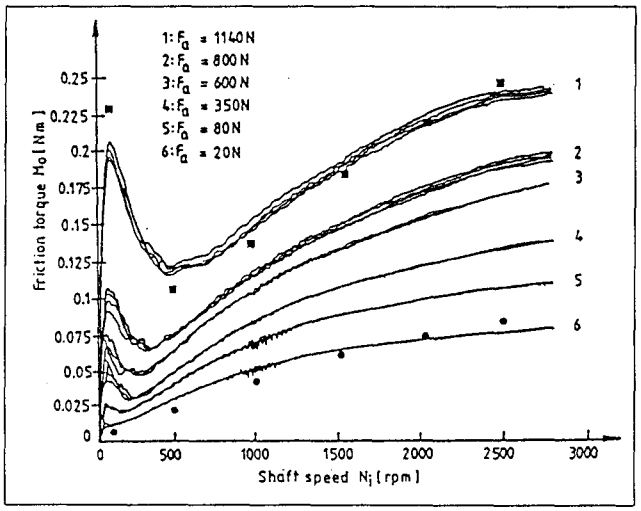

Fig, 4. Friction torque - measurements Predicted values:
■ FQ =1140 N; • FQ = 20N; θ= 30°C

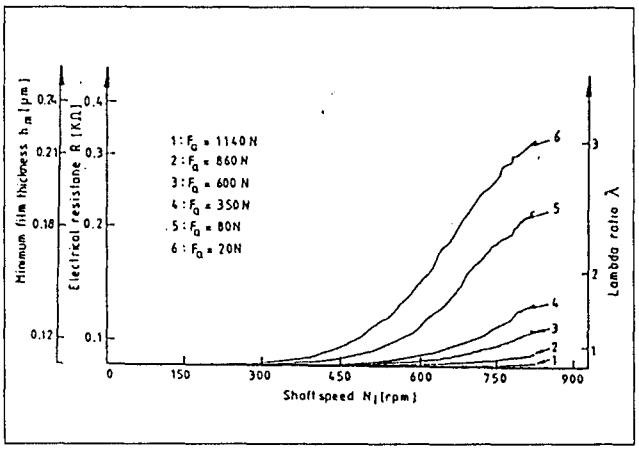

Fig. 5. Measurement of the minimum film thickness
θ = 30°C

Some considerations regarding the influence of both the rotational speed and axial load arc presented in Figure 6 and 7 respectively.

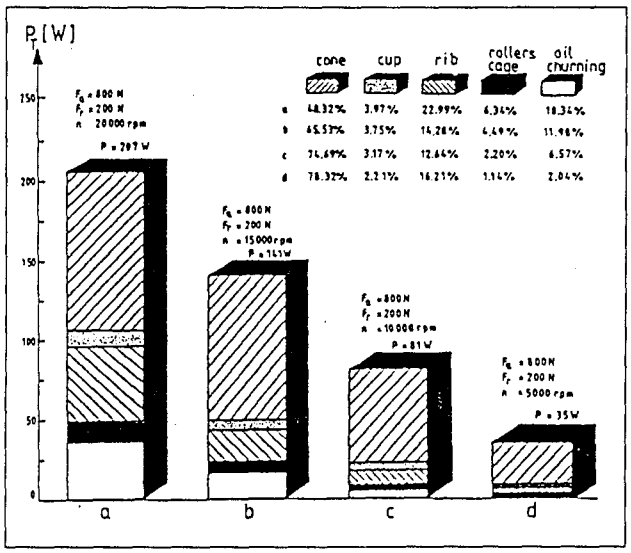

Fig. 6. Friction power loss versus rotation speed

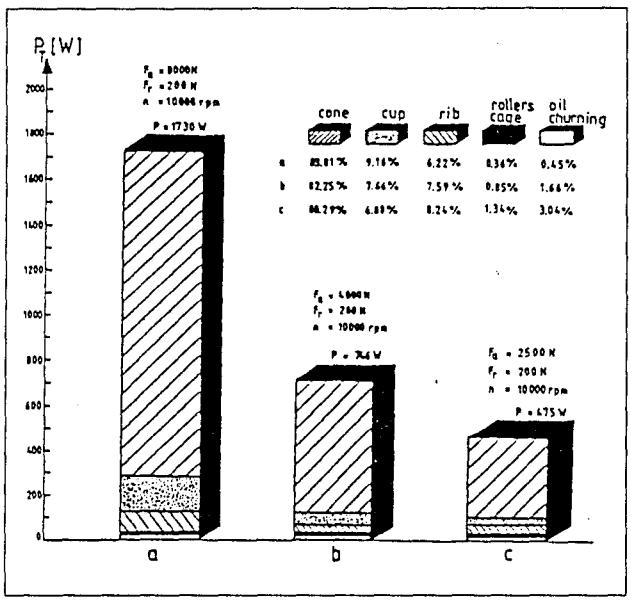

Fig. 7. Friction power loss versus axial load $\eta_0 = 0.08\ Pa{\cdot}s$

The power loss on the inner raceway is higher than that on the outer raceway. It can be noticed that the rollers and cage friction with air - lubricant mixture may represent as much as 20% from the total friction power of the bearing.

5. CONCLUSIONS AND REMARKS

1. To evaluate the friction torques and power loss in a tapered roller bearing, a new analytical model has been developed. The model incorporates the frictional losses in both macro and microcontacts that are realized in a tapered roller bearing.
2. Experimental measurements of the friction torque achieved on the outer ring of tapered roller bearing validated the analytical model. If the tapered roller bearing was working in the low speed domain, the total friction torque versus rotation speed dependence is quite similar with Stribeck's curve from journal bearings applications. It has to be noted that this variation was also mentioned by Zhou [3] and Dalmaz [13], but only for the point contacts between the spherical end roller and inner ring shoulder.
3. A more complete analytical model to evaluate the power losses in a tapered roller bearing was finally developed. With this model, the quantitative contribution of each frictional component in the total power loss can to be evaluated.

6. NOTATIONS

A - contact area, m^2

FA - frictional force due to the asperity contacts, N

FP - pressure or hydrodynamic force, N

FR - rolling resistance force, N

FS - frictional force due to sliding at line contacts, N

F_{ty} - frictional force due to sliding at the rib - roller end contact, N

h_m - minimum film thickness at the rib-roller end contact, mm

M - friction torque, Nm

P - power loss

R - electrical resistance, Ω

Z - number of tapered rollers

τ - shear stress, Pa

Subscripts

i - refers to inner line contact

o - refers to outer line contact

f - refers to rib - roller end contact

c - refers to cage

r - refers to roller

Terminology

cone - inner ring

cup - outer ring

rib - guiding ring of the inner ring

REFERENCES

[1.] SKF - General catalogue, 4000 I IE, Edition 1989

[2.] FAG - Standard Programs, catalogue 41510 EA, Edition 1989

[3.] ZHOU, R. S., HOEPRICH, M. R., **Torque of tapered roller bearing**, Trans. of the ASME, J. of Tribology, vol.113, 1991, p. 590 - 597

[4.] GUPTA, P. K, **On the dynamics of a tapered roller bearing**, Trans. of the ASME, J. of Tribology, vol.2, 1989, p.1- 8

[5.] RACZYNSKI, A, **Effect of working surface shape on power loss in tapered roller bearings**, WEAR, vol. 153, 1992, p. 393 - 400

[6.] WANG, S., CUSANO, S., CONRY, T. F., **A dynamic model of the torque and heat generation rate in tapered roller bearing**, Tribology Transactions, vol. 36, N°4, 1993, p.513 - 524.

[7.] HAMS, T. A, MINDEL, M. H., **Rolling element bearing dynamics**, WEAR, vol. 23, 1973, p. 311- 337

[8.] BERCEA, I., CRETU, S., MITU, N., **A dynamic analysis of tapered roller bearings under fully flooded conditions: Part 1 - Formulation**, WEAR, In press.

[9.] CRETU, S., MITU, N., BERCEA, I., **A dynamic analysis of tapered roller bearings under fully flooded conditions: Part 2 - Results**, WEAR, In press.

[10.] HAMS, T. A., **Rolling bearing analysis**, John Wiley & Sons, New York, second edition, 1984

[11.] HOUPERT, L., **Fast numerical calculations of EHD sliding traction forces; application to rolling bearing**, Trans. of the ASME, J. of Tribology, vol.106, 1984, p. 375 - 385.

[12.] HAMROCK, B.J., DOWSON, D., **Minimum film thickness in elliptical contacts for different regimes of fluid - film lubrication**, Proc. of the 5th Leeds - Lyon symposium, September 1978, p. 22 - 27.

[13.] DALMAZ, G., TESSIER, J. F., DUDRAGNE, G., **Friction improvement in cycloidal motion contacts; rib - roller end contact in tapered roller bearings**, ASGARD - No. 323,1982, p.175 -186.

Teorijska i eksperimentalna studija gukitaka usled trenja u kotrljajnim ležajevima sa koničnim valjcima

U radu je prikazan analitički model za izračunavanje frikcionog momenta i gubitka snage usled trenja u kotrljajnim ležajevima sa koničnim valjcima. Mada se Stribeck-ova kriva obično koristi za primene kod kliznih ležajeva, u radu se pokazuje njena valjanost i za kotrljajne ležajeve sa koničnim valjcima koji rade pri malim ili srednjim brzinama obrtanja.

Ranije publikovan model [8] je dopunjen novim podacima koji objašnjavaju Stribeck-ovu evoluciju za frikcioni moment. Članak ocenjuje izvore trenja, procenjujući učešće svakog izvora u ukupnim gubicima snage.

Теоретический и экспериментальный анализы потерь в результате трения в коническо-роликовых подшипниках качения

В работе показана аналитическая модель расчёта момента трения и потери силы вследствие трения в коническо-роликовых подшипниках качения. Хотя кривая Стрибека обычно используется при расчётах подшипников качения, авторами работы показано, что её можно использовать и для расчётов подшипников качения, работающих при малых и средних оборотах.

Уже опубликовавшая аналитическая модель [8] дополнена новыми данными, обясняющими эволюцию Стрибека в связи с моментом трения. В работе рассматрываются источники трения и оценивается участие каждого в потерях мощности.

UDK 621.833.044.6

B. ROSIĆ, V. LAĆARAC, M. RISTIVOJEVIĆ

ISTRAŽIVANJA

Uticaj raspodele opterećenja na stepen iskorišćenja cilindričnih zupčastih parova

1. UVOD

Sprezanje zupčastih parova karakterisano je kotrljanjem i klizanjem, odnosno trenjem koje se javlja izmedu aktivnih delova bokova spregnutih zubaca. Kako se trenje ne može potpuno eliminisati, to za posledicu ima da se jedan deo energije, koja se prenosi sa pogonskog na gonjeni zupčanik troši na njegovo savlađivanje. Gubici energije koji nastaju u toku sprezanja zupčanika iskazuju se posredstvom bezdimenzionog fakota - stepena iskorišćenja. S obzirom na sve strožije zahteve u pogledu uštede energije, stepen iskorišćenja predstavlja veoma značajnu karakteristiku pri izboru kinematskih i geometrijskih parametara zupčastog para. U dosadašnjim istraživanjima [1,] [4], [5], [6], [7] razmatran je uticaj viskoziteta ulja, brzine klizanja, brzine kotrljanja i hrapavosti na stepen iskorišćenja zupčastog para, uticaj karaktera raspodele opterećenja nije analiziran.

U ovom radu analiziran je uticaj raspodele opterećenja kod istovremeno spregnutih parova zubaca na energetske gubitke zupčastog para.

Doc dr Božidar Rosić,
mr Vesna Laćarac,
Doc dr Mileta Ristivojević
Mašinski Fakultet, Beograd

2. RASPODELA OPTEREĆENJA KOD ISTOVREMENO SPREGNUTIH PAROVA ZUBACA

Da bi se obezbedio kontinualan prenos obrtnog kretanja sa pogonskog na gonjeni zupčanik. neophodno je da pre nego što jedan par spregnutih zubaca završi svoje dodirivanje, sledeći par već započne svoj dodir. Kinematski pokazatelj postojanja kontinualnosti prenosa obrtnog momenta je stepen sprezanja bokova, koji mora biti veći od jedinice. Angažovanjem većeg broja parova zubaca u prenošenju opterećenja zupčastog para, stvorena je mogućnost za odgovarajuću raspodelu opterećenja kod istovremeno spregnutih parova zubaca. U opštem slučaju, ta raspodela opterećenja je neravnomerna, što znači da su pojedini istovremeno spregnuti parovi zubaca različito angažovani u prenošenju ukupnog opterećenja zupčastog para.

Ako se ukupno opterećenje zupčastog para, F_u, prenosi prenosi preko n istovremeno spregnutih parova zubaca, tada su faktori raspodele opterećenja kod pojedinih istovremeno spregnutih parova zubaca odredeni izrazom:

$$K_\alpha = \frac{1}{F_u} I F \qquad (1)$$

gde su: I - jedinična matrica

$F = [F_1\, F_2 \,.\, F_i \,.\, F_n]$ - matrica opterećenja koje prenose pojedini istovremeno spregnuti parovi zubaca

$K_a = [K_{\alpha 1}\, K_{\alpha 1} \,.\, K_{\alpha \iota} \,.K_{\alpha v}]$ - matrica faktora raspodele opterećenja istovremeno spregnutih parova zubaca.

Sa aspekta raspodele opterećenja kod istovremeno spregnutih parova zubaca, mogu se pojaviti dva karakteristič-

na - granična slučaja. Jedan odgovara idealno ravnomernoj raspodeli opterećenja, a drugi izrazito neravnomernoj raspodeli opterećenja. Stvarna - realna raspodela opterećenja nalazi se između ovih ekstremnih raspodela. Kod idealno ravnomerne raspodele opterećenja svi istovremeno spregnuti parovi zubaca podjednako učestvuju u prenošenju ukupnog opterećenja zupčastog para. Da bi ovaj uslov bio ispunjen, potrebno je da srednja linijska opterećenja, duž trenutne linije dodira, istovremeno spregnutih parova zubaca, budu međusobno jednaka:

$$q_1 = \bar{q}_2 = \ldots = \bar{q}_i = \ldots = \bar{q}_n \qquad (2)$$

Na osnovu ove jednakosti, može se pokazati, da se faktor raspodele opterećenja kod istovremeno spregnutih parova zubaca može odrediti samo na osnovu dužine trenutnih linija dodira:

gde su: $B_u = \Sigma B_i$ - ukupna dužina trenutnih linija dodira istovremeno spregnutih parova zubaca

$B = [B_1 B_2 \ldots B_i \ldots B_n]$ - matrica trenutnih linija dodira istovremeno spregnutih parova zubaca.

Tok promene faktora raspodele opterećenja u toku dodirnog perioda, kada se u toku dodirnog perioda smenjuju dvostruka i jednostruka sprega, prikazan je dijagramom na sl. 1-a.

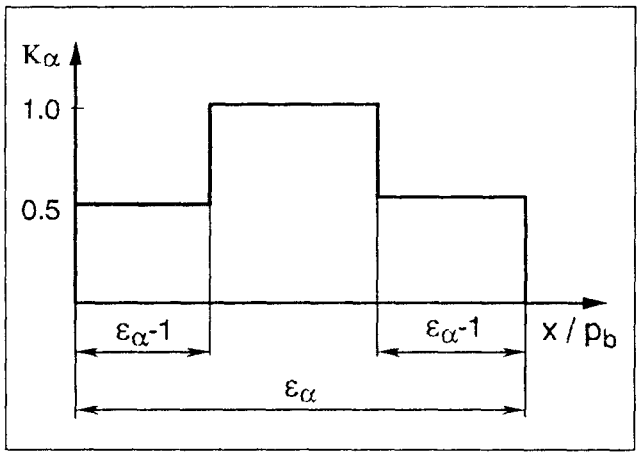

Sl. 1-a. Faktor K_α kod ravnomerne raspodele opterećenja

Kod izrazito neravnomerne raspodele opterećenja, ukupno opterećenje zupčastog para prenosi se samo preko jednog para zubaca. Ako se pretpostavi da *i-ti* par zubaca prenosi ukupno opterećenje zupčastog para, tada je faktor raspodele opterećenja za ostale istovremno spregnute parove zubaca jednak nuli. Jedan primer promene faktora raspodele opterećenja, u toku dodirnog perioda, za slučaj izrazito neravnomerne raspodele prikazan je dijagramom na sl. 1-b.

Kod stvarne - realne raspodele opterećenja, faktor K ima kontinualnu promenu u periodu dvostruke sprege, koja se, obično, aproksimira linearnom promenom, dijagram na sl.1-c.

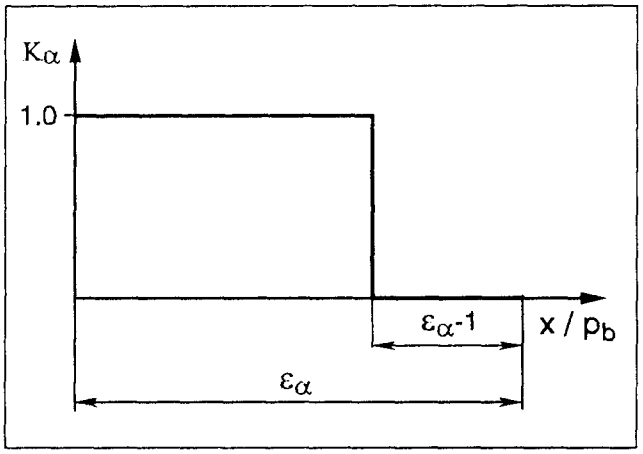

Sl. 1-b. Faktor K_α kod izrazito neravnomerne raspodele opterećenja

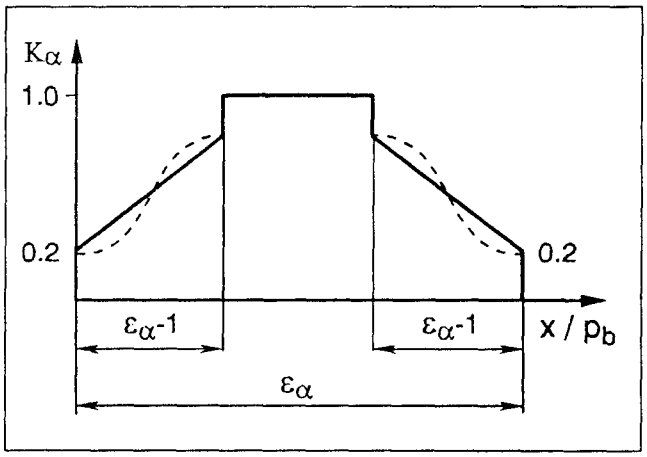

Sl. 1-c. Faktor K_α kod neravnomerne raspodele opterećenja

3. MATEMATIČKI MODEL ZA ODREĐIVANJE STEPENA ISKORIŠĆENJA

Pri prenošenju snage (kretanja i obrtnog momenta) sa pogonskog na gonjeni zupčanik, jedan deo snage se gubi na savlađivanje otpora trenja klizanja i kotrljanja. Intenzitet sile trenja zubaca određuje se na osnovu poznatog izraza:

$$F(x) = \mu(x) \cdot F(x) \qquad (3)$$

Promena koeficijenta trenja, u toku dodirnog perioda, po Benedikt Keliju data je izrazom:

$$\mu(x) = 0.0127 \cdot \left[log \left(\frac{29.66}{B} \cdot F_n \cdot K_{\alpha x} \right) - (\eta \cdot V_{klx} \cdot \bar{V}_{ko}^2) \right] \qquad (4)$$

gde su: F_n - normalna sila koju prenose istovremeno spregnuti parovi zubaca

K_{ax} - faktor raspodele opterećenja za posmatrani par zubaca u nekoj tački dodira

V_{klx} - brzina klizanja profila posmatranog para zubaca u nekoj tački dodira

$\bar{V}_{ko}$ - srednja vrednost brzine kotrljanja profila posmatranog para zubaca u toku dodirnog perioda

B - dužina trenutne linije dodira

η - dinamička viskoznost ulja.

Intenzitet sile trenja kotrljanja koja se javlja na mestu dodira spregnutih parova zubaca:

$$F_k(x) = C \cdot h(x) \cdot B \qquad (5)$$

Promena debljine uljnog sloja, u toku dodirnog perioda, po Higinsu, data je izrazom:

$$h(x) = 1.6 \cdot \alpha^{0.6} \cdot (\eta \cdot V_{ko})^{0.7} \cdot E^{0.003} \cdot R_x^{0.43} \cdot (F_N \cdot K_{ax})^{-0.13} \qquad (6)$$

gde su: α - piezo koeficijent viskoznosti
E - redukovani modul elastičnosti
R_x - srednji poluprečnik krivine profila posmatranog para zubaca u nekoj tački dodira
$C = 9 \cdot 10^7\ N/m^2$

Na sl. 2 prikazana su opterećenja koja deluju na istovremeno spregnute parove zubaca u periodu dvostruke sprege (F_m, F_k, F_n) pri prenošenju obrtnog momenta i kretanja sa pogonskog zupčanika (T_1, ω_1) na gonjeni zupčanik (T_2, ω_2). Uvođenjem pretpostavke o stacionarnosti obrtnog momenta na pogonskom zupčaniku i radnog prenosnog odnosa. sledi da je

$$T_1 = const; \quad i = const \qquad (7)$$

Posmatrajući ravnotežu pogonskog zupčanika, za osu O_1 pod dejstvom opterećenja koja su prikazana na sl. 2 respektujući pri tome jednačine (3), (4), (5) i (6) i uslov (7) dolazi se do ukupne normalne sile koja deluje na istovremeo spregnute parove zubaca. Izrazi za određivanje ove sile. u odgovarajućim oblastima dodirnog perioda, dati su u tabeli I.

Za određivanje stepena iskorišćenja zupčastog para u svakoj tački dodira profila istovremeno spregnutih paro-

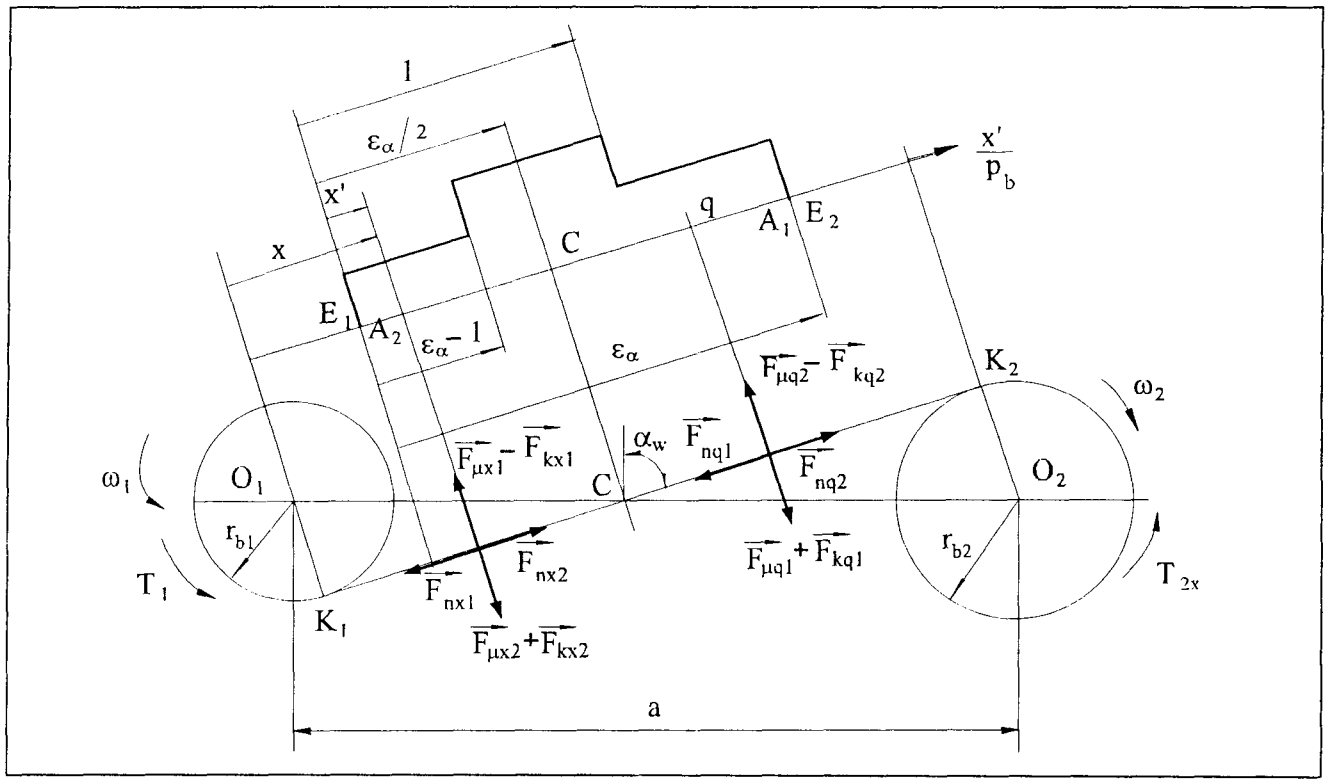

Sl. 2. Šema opterećenja kod istovremeno spregnutih parova zubaca

Tabela 1.

x'	F_N	
$0 \ldots (\varepsilon_\alpha - 1)$	$\dfrac{T_1 - (F_{k1q} \cdot p_b + x \cdot F_{k1q} + F_{kx1} \cdot x)}{r_{b1} + K_{aq} \cdot \mu_q \cdot (x + p_b) - K_{ax} \cdot \mu_x \cdot x}$	$q = x - p_b$
$(\varepsilon_\alpha - 1) \ldots \varepsilon_\alpha/2$	$\dfrac{T_1 - F_{kx1} \cdot x}{r_{b1} - \mu_x \cdot x}$	
$e_\alpha/2 \ldots 1$	$\dfrac{T_1 - F_{kx1} \cdot x}{r_{b1} + \mu_x \cdot x}$	
$1 \ldots \varepsilon_\alpha$	$\dfrac{T_1 - F_{k1q} \cdot (x - p_b) - F_{kx1} \cdot x}{r_{b1} + K_{aq} \cdot \mu_x \cdot x - K_{aq} \cdot \mu_q \cdot (x - p_b)}$	$q = x - p_b$

va zubaca, tzv. trenutna vrednost stepena iskorišćenja, potrebno je poznavati i trenutne vrednosti obrtnog momenta na gonjenom zupčaniku (T_{2x}). Posmatranjem ravnoteže gonjenog zupčanika, za osu O_2, pod dejstvom opterećenja koja su prikazaxia na sl. 2, respektujući pri tome jednačine (3), (4), (5) i (6) i uslov (7) i izraze za ukupnu normalnu silu iz T1, dolazi se do trenutne vrednosti obrtnog momenta na gonjenom zupčaniku (T_{2x}). Pregled izraza za odredivanje ovog obrtnog momenta, u odgovarajućim oblastima dodirnog perioda, prikazan je u tabeli 2.

Formirani model omogućuje odredivanje stepena iskorišćenja zupčastog para u svakoj tački dodira spregnutih profila zubaca, odnosno "trenutne" vrednosti stepena iskorišćenja, kada se kinematski pol nalazi na sredini dodirnog perioda.

$$\eta_x = \frac{T_{2x}}{T_1} \cdot \frac{1}{i}$$

Stepen iskorišćenja zupčastog para u toku dodimog perioda, tzv. efektivni stepen iskorišćenja, određen je izrazom:

$$\eta_{ef} = \frac{1}{\varepsilon_\alpha \cdot m \cdot \pi \cdot \cos\alpha} \cdot \int_E^A \eta_x \cdot dx$$

gde su: m - modul zupčastog para

α - ugao nagiba profila alata osnovne zupčaste letve

ε_α - stepen sprezanja profila.

Tok promene "*trenutnih*" vrednosti stepena iskorišćenja, cilindričnog zupčastog para, u toku dodirnog perioda prikazan je na sl. 3a, 3b, 3c, za karakteristične slučajeve raspodele opterećenja kod istovremeno spregnutih parova zubaca. Kod ravnomerne raspodele opterećenja trenutne vrednosti stepena iskorišćenja u oblasti dvostruke sprege imaju približno istu vrednost u svakoj tački dodira sl.3a. Trenutne vrednosti stepena iskorišćenja, kod neravnomerne raspodele opterećenja, u oblasti dvostruke sprege menjaju se po paraboličnom zakonu, sl 3b, a kod izrazito neravnomerne raspodele opterećenja menjaju se po linearnom zakonu, sl. 3c. U oblasti jednostruke sprege trenutne vrednosti stepena iskorišćenja

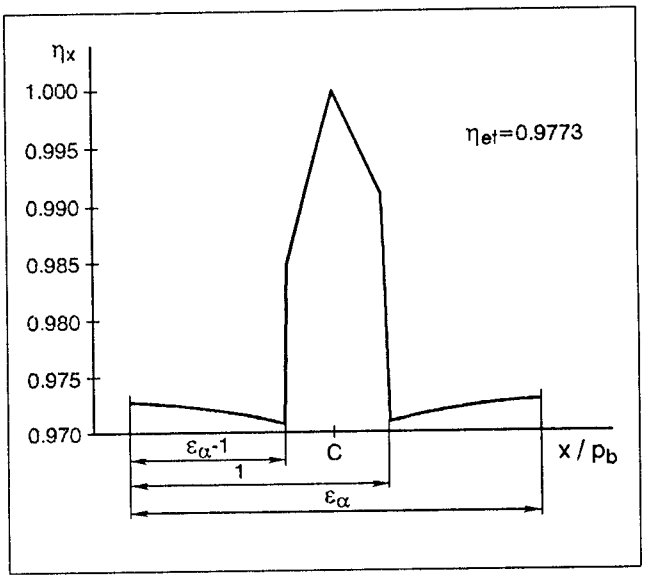

Sl. 3a Trenutne vrednosti stepena iskorišćenja kod ravnomerne raspodele opterećenja

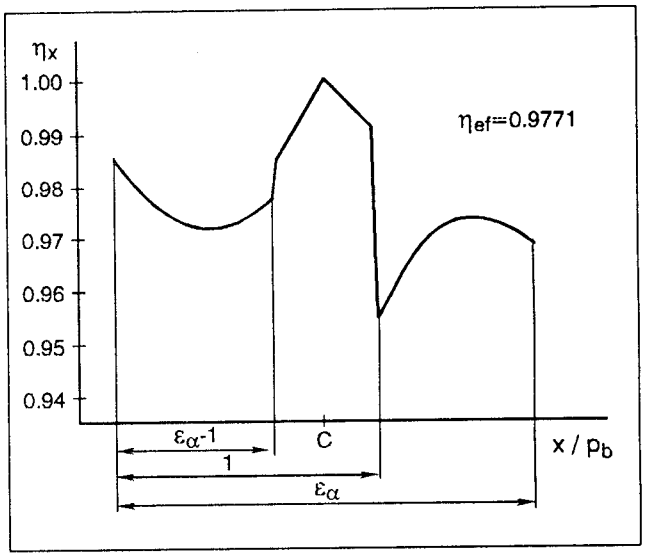

Sl. 3b Trenutne vrednosti stepena iskorišćenja kod izrazito neravnomerne raspodele opterećenja

menjaju se po linearnom zakonu. Pri tome, na granicama prelaska dvostruke sprege u jednostruku i jednostruke sprege u dvostruku, trenutne vrednosti stepena iskorišćenja imaju skokovitu promenu, sl 3a, 3b i 3c. Stepen iskorišćenja maksimalnu vrednost dostiže u kinematskom polu, što ukazuje na činjenicu da su otpori kotrljanja znatno manji od otpora klizanja.

Tabela 2.

X'	F_N
$0 \ldots (\varepsilon_\alpha - 1)$	$F_N \cdot r_{b2} + (F^q_{\mu 2} - F^q_{k2}) \cdot \left[a \cdot \sin\alpha_w - (x + p_b) \right] - (F^q_{\mu 2} - F^q_{k2}) \cdot (\sin\alpha_w - x)$
$(\varepsilon_\alpha - 1) \ldots \varepsilon_\alpha/2$	$F_N \cdot (r_{b2} - \mu_x \cdot (a \cdot \sin\alpha_w - x)) - F_{k2x} \cdot (a \cdot \sin\alpha_w - x))$
$e_\alpha/2 \ldots 1$	$F_N \cdot (r_{b2} + \mu_x \cdot (a \cdot \sin\alpha_w - x)) - F_{k2x} \cdot (a \cdot \sin\alpha_w - x))$
$1 \ldots \varepsilon_\alpha$	$F_N \cdot r_{b2} + (F_{\mu 2} - F_{k2}) \cdot (a \cdot \sin\alpha_w - x) - (F_{\mu 2} + F_{k2}) \cdot (\sin\alpha_w - x + p_b)$

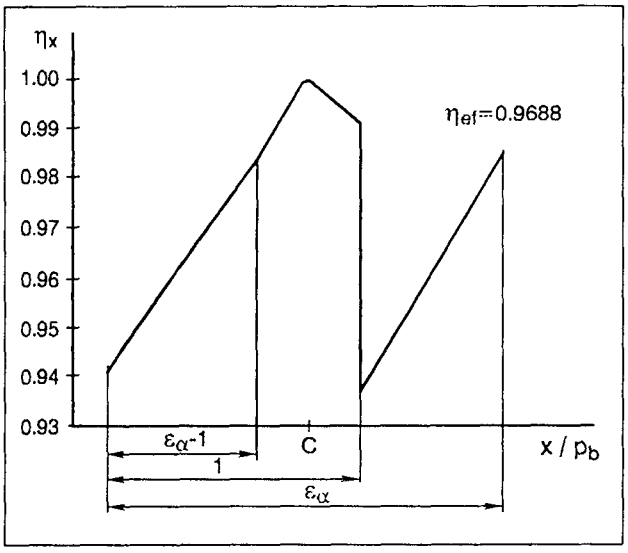

Sl. 3c Trenutne vrednosti stepena iskorišćenja kod neravnomerne raspodele opterećenja

4. ZAKLJUČAK

Na osnovu sprovedene analize sledi da tok promene trenutnih vrednosti stepena iskorišćenja zavisi od karaktera raspodele opterećenja kod istovremeno spregnutih parova zubaca. Sa aspekta stepena iskorišćenja zupčastog para treba težiti što ravnomernijoj raspodeli opterećenja. Sa porastom neravnomernosti raspodele opterećenja, stepen iskorišćenja se smanjuje. Pri tome, minimalni gubici energije javljaju se u kinematskom polu, što pokazuje da su gubici energije usled otpora kotrljanja zanemarivo mali.

Formirani model i kompjuterski program omogućuju da se variranjem: parametara ozubljenja, intenziteta opterećenja, preciznosti izrade, zatim načina i sredstva za podmazivanje, dođe do najpovoljnije konstrukcije prenosnika koja treba da ispuni veoma stroge zahteve u energetskom pogledu.

LITERATURA

[1.] DOWSON D., HIGGINSON G. R., **Elastohydrodynamic Lubrication**, S.I. Edition 1977. Pergamon Press Ltd, p.190

[2.] RISTIVOJEVIĆ M., **Analiza raspodele opterećenja na istovremeno spregnute parove zubaca sa primenom na čvrstoću zupca zupčanika**, magistarski rad, Mašinski fakultet, Beograd,1985.

[3.] ROSIĆ B., **Istraživanje i optimizacija parametara unutrašnjeg ozubljenja planetnih prenosnika**, doktorska disertacija, Beograd, 1992.

[4.] ANDERSON N. E., LÖWENTHAL S. N., **Design of Spur Gears for Improved Efficiency**, ASME. Vol. 104, 1982

[5.] NIEMANN G., STOBEL K., **Reibungszahlen bei elastohydrodynamischer Schmierung in Reibrad und Zahnradgetrieben**, Konstruktion, 1971, 23, 7

[6.] JARCHOW F., DIERICH H., **Weiterentwicklung der Theorie zur Ermittlung von Hertzschen Drucken Reibungszahlen und Vergleichsspannungen in Verzahnungen von Schneckentrieben**, Konstruktion,1991, 43, pp 117-123

[7.] WINTER H., OSTER P., **Beanspruchung der Zahnflanken unter EHD-Bedingungen**, Konstruktion,1981, 33, pp 421-434

Influence of The Loading Distribution on The Efficiency Ratio of The Cylindrical Tooth Couples

In the paper is analyzed the influence of the loading distribution for simultaneously coupled tooth pairs on the efficiency ratio of the cylindrical evolvent tooth couples. The mathematical model was formed and the computer program was developed for determination of the instantaneous and effective value of the efficiency ratio when, in the coupling period are alternating the unilateral and bilateral coupling. Results are presented in the form of diagrams for instantaneous values of the efficiency ratio during the coupling period and the values of the effective efficiency ratio are calculated.

Влияние распределения нагрузки на степень использования цилиндрических зубчатых пар

В работе анализируется влияние распределения нагрузки одновременно сопряжённых пар зубьев на степень использованния цилиндрических эвольвентных зубчатых пар. Авторами построена математическая модель и развита вычислительная программа, определяющая мгновенные и эффективные значения степени использования в течение контакта, при котором чередуются двойное и однозаходное зацепление. Результаты показаны в форме эпюры для мгновенных значений степени использования в течение контакта и подсчитана эффективная степень использования.

UDK 621.833.044.6

M. ZLATANOVIĆ, A. RAC,
D. GERZIĆ, A. KUNOSIĆ

Ispitivanje tribosistema za pumpe visokog pritiska

1. UVOD

Procenjuje se, da se u industrijski razvijenim zemljama za pogon raznih pumpi troši otprilike 10% ukupno proizvedene energije, a u okviru energetske potršnje procesne industrije ovaj procent se kreće i do 20%. [1]. Značajno povećanje efikasnosti rada i smanjenje energetske potrošnje pumpi može se postići površinskom obradom pokretnih vitalnih delova pumpe. Danas postoji čitav niz tehnoloških postupaka za obradu površine materijala, koji obezbeđuju efikasniji i pouzdaniji rad funkcionalnih sklopova, smanjuju energetsku potrošnju usled trenja i troškove zbog zastoja uređaja usled otkaza [2].

U istraživanju je postavljen problem izbora najpogodnijeg materijala, nama dostupnog na tržištu, za vitalne elemente hidropumpi visokog pritiska. Tolerancija dimenzija cilindra i klipa, koji čine jedan tribološki par, kritična je za rad pumpe te je neophodno za njen visoki učinak da habanje bude minimalno. U suprotnom, ako se zazor između kućišta (cilindra) i klipa poveća, drastično se povećavaju gubici i opada stepen korisnosti.

M. Zlatanović, Elektrotehnički fakultet, Beograd
A. Rac, Mašinski fakultet, Beograd
D. Gerzić, Elektrotehnički fakultet, Beograd
A.Kunosić, Institut Mihailo Pupin, Beograd

2. EKSPERIMENTALNI POSTUPCI

2.1 Izbor materijala za prevlake i metode nanošenja

Za izradu ispitnih uzoraka - parova trenja koristili smo:

- NL50 nodularni liv i Č.4531 za nitriranje, za ispitne diskove *100mm;
- Č.4146 čelik za ležajeve i Č.1221 konstrukcioni čelik za ispitne pinove sa kalotom *8mm.

Za formiranje prevlaka i slojeva na ispitnim uzorcima primenjeni su materijali i odgovarajući postupci površinske obrade (tabela 1):

- praškaste tvrde legure NiCr - raspršivanje u acetilenskom plamenu (Lurgi uređaj);
- tvrdi hrom - metoda elektrohemijske depozicije iz rastvora;
- nitrid gvožđa (Fe4N) - plazma nitriranje [3,4,5], (uređaj JONEL-MONO5).

2.2 Ispitivanje parova trenja

Celokupna ispitivanja izabranih uzoraka parova materijala vršena su u uslovima čistog klizanja pri podmazivanju, u približnim uslovima realne primene:

- brzina klizanja 2 m/s;
- opterećenje - sila: 60, 80, 100, 120 i 140 N;
- približna vrednost pritiska: 1820, 2000, 2160, 2420 MN/cm^2;
- vrsta maziva: hidraulično ulje "Hidraol 50";
- temperatura maziva 400C;
- sobna temperatura, atmosferski uslovi.

Tabela 1: Materijali za prevlake

Naziv	Hemijski sastav	Debljina prevlake	Tvrdoća
Prevlaka na bazi hroma, Cr	Cr - 100	80 μm	980 $HV_{0,025}$
Prevlaka na bazi legure nikla, (NiCr)	Ni -74, B -3,0, Fe -4,75 Cr -13,5, Si -4,25	0,2 - 0,3 mm	620 - 690 $HV_{0,05}$
Prevlaka na bazi legure gvožđa, (nitrid gvožđa - Fe_4N)	Fe_4N - 100	5 μm	1000 $HV_{0,002}$

2.3 Ispitivani uzorci parova materijala na uređaju Tribometar 62 "pin-disk"

Materijali, kao i geometrijski oblik spregnutih delova , izabrani su tako da simuliraju uslove dodira koji se ostvaruju u predviđenoj realnoj konstrukciji hidropumpe. Kalota epruvete (pina), koja je u stalnom dodiru sa diskom, izložena je habanju. Kombinacije parova materijala i prevlake koje su korišćene pri ispitivanju prikazane su u tabeli 2.

Iz tabele 2 sledi da su za izradu diska korišćena dva materijala: sivo liveno gvožđe sa nodularnim grafitom (NL50) i čelik Č.4531 čija je površina obrađena postupkom plazma nitriranja (Č.4531+ Fe4N).

Tabela 2: Ispitivani uzorci

Uzorak	Kalota	Disk
I	Č.4146	NL50
II	Č.4146+Cr	NL50
III	Č.1221+NiCr	NL50
IV	Č.4146	Č.4531+Fe4 N

Kalote epruveta kod uzoraka I i IV izrađenih od čelika Č.4146 su bez prevlake, dok je kod uzorka II na kalotu naneta prevlaka na bazi hroma (Č.4146 + Cr). Kod uzorka III kalota je izrađena od čelika Č.1221 sa prevlakom na bazi legure nikl-hrom (Č.1221 + NiCr).

Tabela 3: Hrapavost površina

Materijal	Ra [μm]
Disk NL50	0.089 - 0.192
Disk Č.4531+Fe4N	0.012 - 0.032
Kalota Č.4146	0.02 - 0.04
Kalota Č.4146+Cr	0.15 - 0.40
Kalota Č.1221+NiCr	0.02 - 0.04

U tabeli 3 prikazane su vrednosti srednjeg aritmetičkog odstupanja profila R_a za pojedine materijale i prevlake. Merenje strukturnih parametara površina trenja i dijagrama hrapavosti traga habanja vršena su na uređaju TALYSURE 6.

3. REZULTATI ISPITIVANJA

Karakteristike trenja i habanja ispitivanih uzoraka materijala prikazane su preko dijagrama na slikama od 1 do 6.

Na slici 1 data je zavisnost koeficijenata trenja od opterećenja za sve ispitivane uzorke materijala. Pri tome su, kao karakteristične veličine, uzete srednje vrednosti koeficijenata trenja nakon perioda uhodavanja.

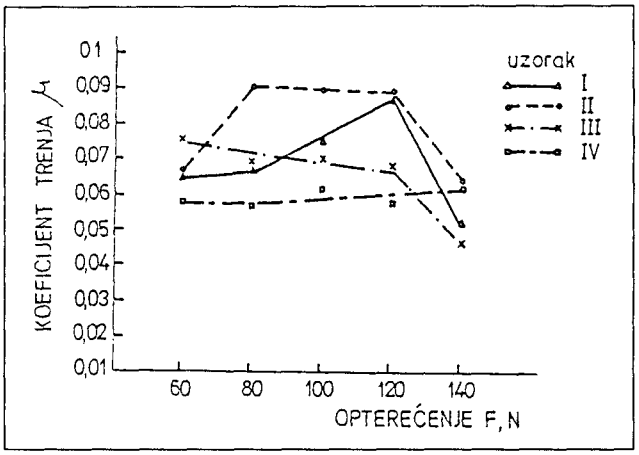

Sl. 1. Zavisnost koeficijenta trenja od opterećenja

Slika 2 predstavlja ilustraciju zavisnosti veličine habanja za uzorak IV, iskazane kao srednji prečnik habanja kalote u funkciji pređenog puta i to za sva korišćena opterećenja.

Zavisnost srednjeg prečnika habanja kalote, za ispitivane parove materijala, od veličine opterećenja prikazana je na slici 3.

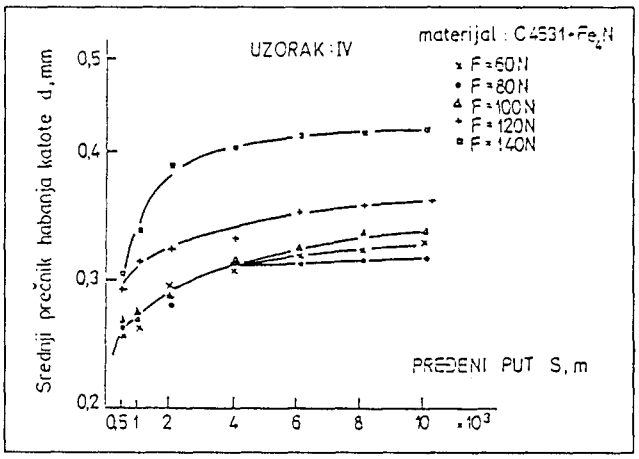

Sl. 2. Zavisnost habanja od pređenog puta

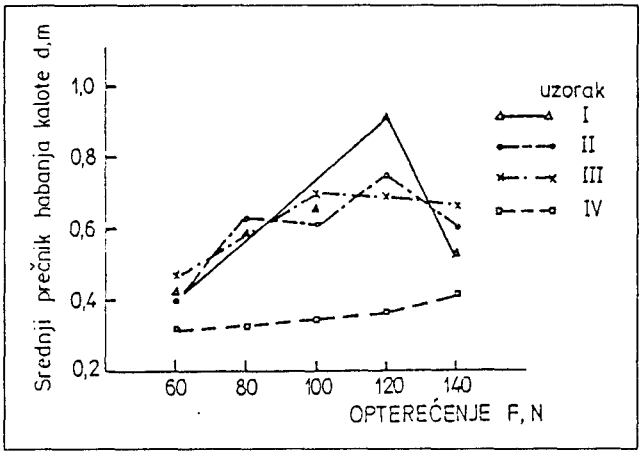

Sl. 3. Zavisnost srednjeg prečnika habanja od opterećenja

Količina materijala uklonjenog habanjem sa kalote i diska za posmatrani par materijala ocenjivana je i upoređivana na osnovu merenja dubine traga habanja. Dubina traga habanja određena je dijagramom hrapavosti tragova habanja. Kao mera habanja korišćena je veličina I_h - intenzitet habanja, koja predstavlja odnos maksimalne dubine pohabane površine izražene u mikrometrima i pređenog puta iskazanog u metrima. Ovako određen intenzitet habanja prikazan je, za svaki uzorak posebno, na slici 4 (a, b, c i d). Na slici 5 (a, b i c) uporedo su prikazani intenziteti habanja pri opterećenjima od 80, 100 i 120 N, za materijale koji su bili predmet razmatranja. Takođe su, za napred navedena opterećenja, na slici 6 (a, b i c) date promene koeficijenta trenja tokom ispitivanja, odnosno u funkciji pređenog puta.

4. DISKUSIJA REZULTATA

Na osnovu dobijenih rezultata ispitivanja mogu se izneti sledeća zapažanja:

Veličina koeficijenta trenja kod uzoraka I i II, kada se posmatra u funkciji opterećenja (slika 1), leži u granicama od 0,065 do 0,09. Kod ovih uzoraka zapaža se određeno rasipanje rezultata. Značajno pravilniji rezultati su dobijeni za uzorak III, kod koga sa porastom opterećenja koeficijent trenja opada (od 0.068 do 0.048). Kod uzorka IV koeficijent trenja raste sa porastom opterećenja. U ispitivanoj oblasti opterećenja koeficijent trenja je u granicama od 0.055 do 0.063. Zavisnost koe-

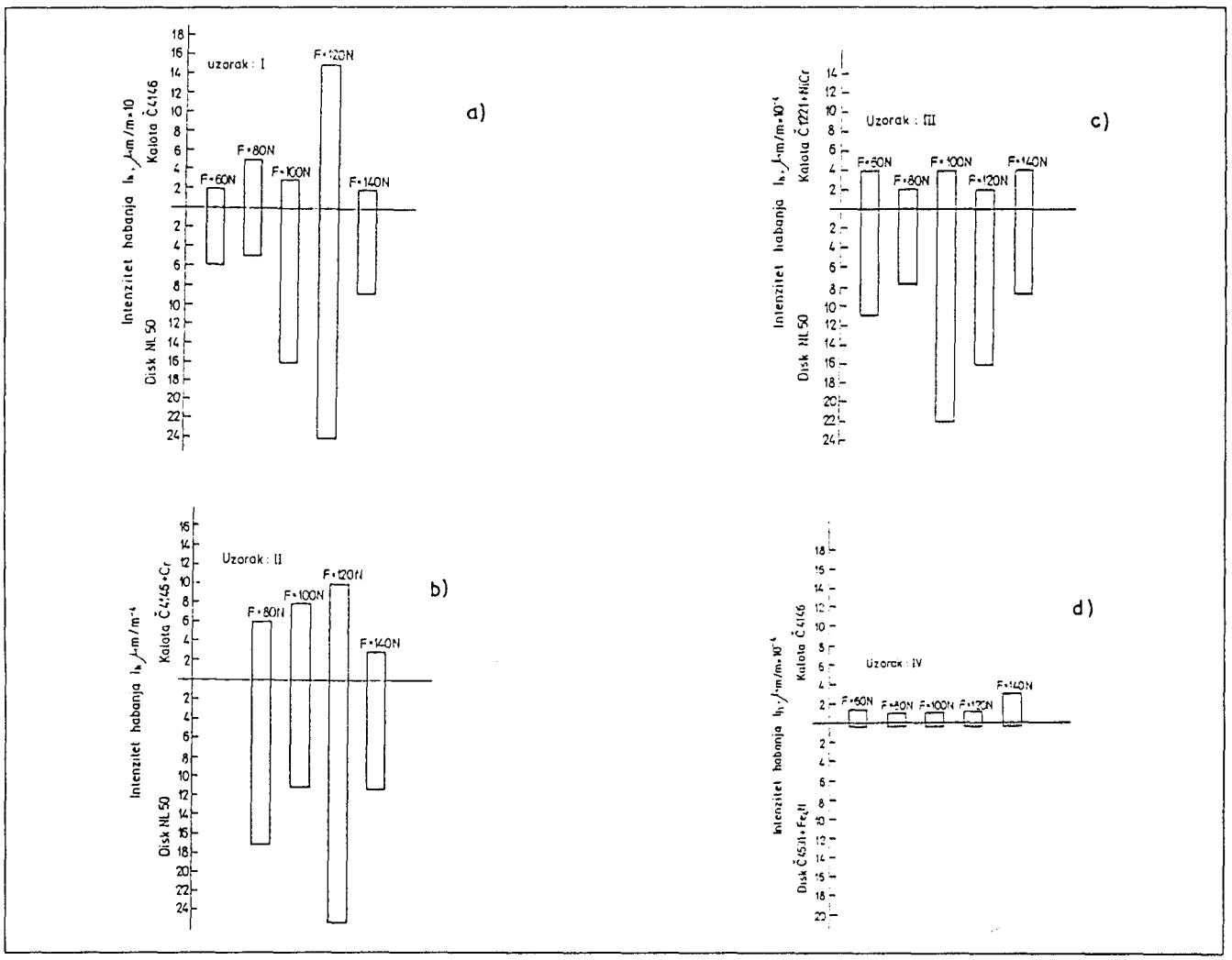

Sl. 4. Zavisnost intenziteta habanja od opterećnja

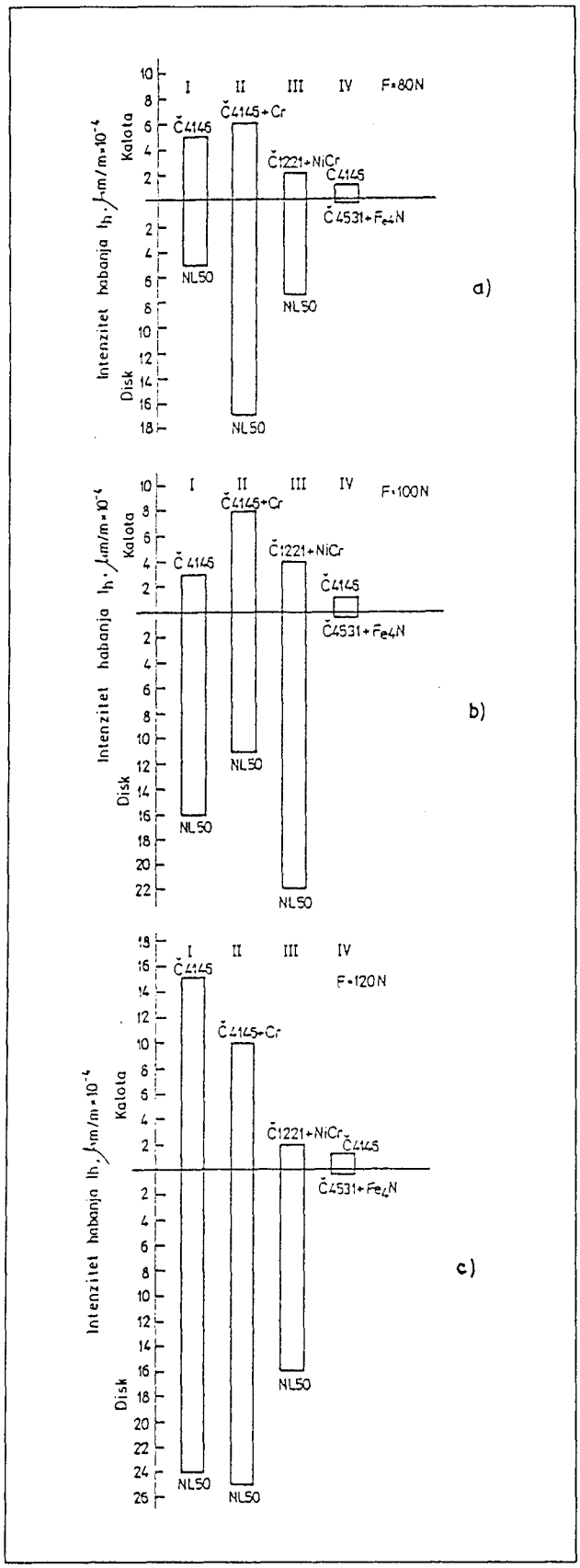

Sl. 5. Upoređenje intenziteta habanja za sve triboparove

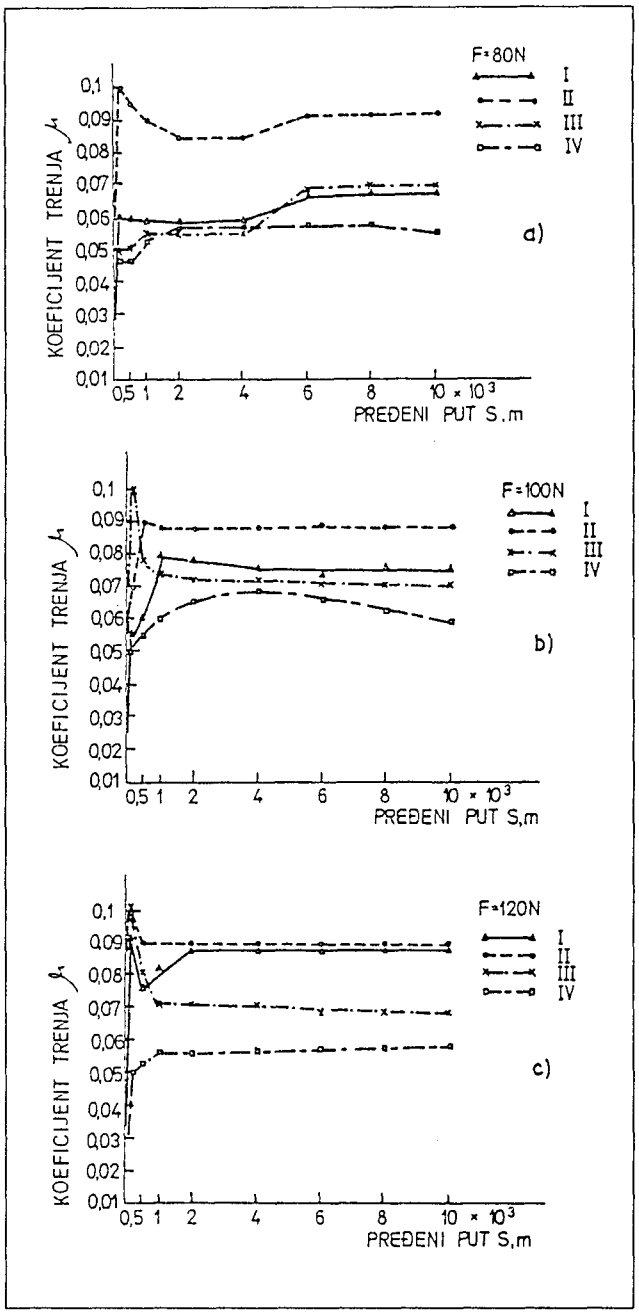

Sl. 6. Zavisnost koeficijenta trenja od pređenog puta

ficijenta trenja od pređenog puta (slika 6) pokazuje da, kod svih uzoraka, posle određenog puta dolazi do stabilizacije, što je povezano sa periodom prilagođavanja površina.

Veličina habanja kalote kod uzoraka I, II i III, izražena preko prečnika habanja, ne pokazuje zadovoljavajuću pravilnost (slika 3). Odstupanja i rasipanje rezultata kod posmatranih uzoraka su, kao i kod koeficijenta trenja, po mišljenju istraživača, posledica netačnosti pri izradi kalote i neadekvatnog nanošenja prevlaka.

Rezultati habanja, dobijeni merenjem dubine traga habanja a izraženi kao intenzitet habanja I_h (slika 4), takođe pokazuju određeno rasipanje razultata. Od ovog odstupaju samo rezultati dobijeni kod uzorka IV, koji imaju jasnu teorijsku opravdanost. Kod ovog uzorka, odnosno korišćenih materijala, uočava se period uhodavanja (slika 2) koji traje 2000 do 4000 metara. Istovremeno, rezultati pokazuju da izabrani par materijala u uzorku IV ima najmanje habanje i da, sa porastom

opterećenja, habanje kalote blago raste (slika 3), pri čemu je habanje diska neznatno i skoro nezavisno od opterećenja, u opsegu u kome je vršeno ispitivanje. Ova činjenica ukazuje na to da prevlaka dobijena postupkom plazma nitriranja (nitrid gvožđa) u dodiru i klizanju sa čelikom Č.4146 daje pogodnu kombinaciju za parove trenja.

5. ZAKLJUČAK

Istraživanje je imalo za cilj da nađe put za rešenje tribopara - elemenata pumpi visokog pritiska, sa gledišta izbora pogodnih materijala koji zadovoljavaju tehničke zahteve funkcionalnih sklopova.

U tom cilju izvršena su brojna laboratorijska ispitivanja prevlaka od:

- legure na bazi nikla i hroma;
- čistog metala hroma;
- slojeva nitridnih jedinjenja gvožđa;

u kontraparu sa materijalima: nodularnim sivim livom NL50 i čelikom za kotrljajuće ležajeve Č.4146.

Geometrijski oblik ispitnih parova trenja izabran je tako da simulira uslove dodira u realnoj konstrukciji.

Spoljni mehanički parametri, koji determinišu uslove procesa klizanja i habanja u sistemu, identični su za sve ispitne materijale i približni su realnim uslovima rada u konstrukciji.

Metode koje smo koristili za formiranje kliznih površina tribopara spadaju u savremene tehnološke postupke za obradu površina sa specijalnim svojstvima:

- termoraspršivanje;
- elektrohemijsko nanošenje;
- plazma nitriranje.

Analiza trenja i habanja vršena je pomoću testa "pin na disku", u laboratoriji Mašinskog fakulteta u Beogradu. Relativna brzina kretanja pina i diska i opterećenje birani su u opsegu koji odgovara eksploatacionim uslovima rada delova pumpi. Na slici 1 prikazani su rezultati merenja promene koeficijenta trenja u funkciji sile normalne na kontaktnu površinu, za sva četiri tribopara. Najmanja varijacija koeficijenta trenja primećena je kod tribopara IV, iz čega proizilazi da je ovaj sistem najpogodniji za praktičnu primenu iako, pri najvećem opterećenju, drugi triboparovi pokazuju nešto niži koeficijent trenja.

Intenzitet habanja varira u zavisnosti od površinske obrade materijala i najmanji je za slučaj tribopara IV: kalota od čelika Č.4146 i plazma nitrirani disk od čelika Č.4531.

LITERATURA

[1.] *Jantainen, E., Miettinen, J. and Ollila, H.*, **Maintenance and Downtime Costs of Centrifugal Pumps i Finish Industry**, 13th Int. Pump Tech. Conf. - Pumps for Safer Future, London, April 1994., p. 11

[2.] *Holmberg, K. and Matthews, A.*, **Coating Tribology**, Elsevier, 1994.

[3.] *Zlatanović, M. and Stošić, P.*, **Comparative Tests of TiN and Ti0.5Al0.5N Coated Hobs in Gear Cutting Operations**, Vacuum, Vol. 36, 6(1989), pp. 557-562

[4.] *Zlatanović, M. and Munz, W. D.*, **Wear Resistence of Plasma Nitrided and Sputter Ion Plated Hobs**, Surface & Coatings Technology, 48(1990), pp. 17-30

[5.] *Zlatanović, M., Kakaš, D., Mažibrada, Lj., Kunosić, A. and Munz, W. D.*, **Influence of Plasma Nitriding on Wear Performance of TiN Coating**, Surface & Coatings Technology, 64(1994) pp. 173-181

Testing of The Tribosystems for High Pressure Pumps

Abstract. In the paper are presented results of testing the characteristics of the tribological system - friction pairs for the high pressure pumps. For making the friction pairs are used the following materials: NL50, Č. 4146, Č. 1121 and Č. 4531 in combination with the surface modified contra bodies. Applied are the plasma nitriding procedure, flame dispersion process and electronic deposition.

Four tribological pairs were tested, and it turned out that the best characteristics for application in high pressure pumps, with respect to the friction coefficient and the wear amount, has the tribological pair whose one element is made of Č. 4146 towards the plasma nitriding contra body made of Č. 4531.

Исследование трибосистем для насосов высокого давления

В работе изложены результаты исследований характеристик трибологических систем - трущихся пар для насосов высокого давления. Для изготовления трущихся пар использовали материалы НЛ50, Ч.4146, Ч.1121 и Ч.4531 в сочетании с поверхностно обработанными контртелами. При этом использовали плазменное нитрирование, пламенное распыление и электрохимическое накопление.

В течение исследования испытывали четыре трибологические пары. Полученные результаты показывают, что с точки зрения коэффициентов трения и изнашивания, наиболее удобной оказывается трибологическая пара один элемент которой сделан из Ч.4146, а контртело из Ч.4531, обработанное плазменным нитрированием.